EXPERIMENTS WITH UNCONVENTIONAL CROSSFLOW HEAT EXCHANGERS

Thesis by

Edward Kenneth Ruth

In Partial Fulfillment of the Requirements

For the Degree of

Doctor of Philosophy

California Institute of Technology

Pasadena, California

1981

(Submitted July, 1980)

ACKNOWLEDGEMENTS

A great number of people made this thesis possible. The single most important one is Professor W. D. Rannie whose ideas and advice are the cornerstone of this work. I am also grateful for the suggestions of Professor Edward Zukoski.

A special thanks must also go to George Lundgren and the men of the Aeronautics machine shop: Howard McDonald, Robert Seguine, and George Willson for all the advice, help, and friendship they have given me.

I would also like to show my appreciation to Frank Linton and Victor Jaramillo for their help on the experiment and to Dorothy Eckerman for her typing of the manuscript.

I am grateful for the financial support provided by the California Institute of Technology and the United States Department of Energy.

Mr. Shawn Hall has been a steady source of friendship and support all of my years at Caltech and I shall always be indebted to him and appreciative of his friendship.

Finally I would like to dedicate this work to my parents for all the love that they have given me.

ABSTRACT

These experiments consisted of measurements of pressure losses and heat transfer rates for two unconventional crossflow heat exchanger configurations.

The first type consisted of an arrangement of circular tubes in a sawtooth pattern. Performance of this type did not appear to be an improvement over more conventional heat exchangers.

The second type used exchanger tubes of a special lenticular cross section so spaced as to keep the velocity of the fluid flowing outside the tubes nearly constant in magnitude reducing separation and drag. The lenticular tubes' performance was superior to the conventional types, especially at higher Reynolds numbers.

SUMMARY

The purpose of these experiments was to investigate the performance of two unconventional crossflow heat exchanger configurations to determine if these might lead to a decrease in the pressure loss of the flow through the heat exchanger for a given heat transfer rate.

It is difficult to compare different types of heat exchangers without considering the design requirements of their intended applications. In this work the ratio of friction coefficient to heat transfer coefficient in the dimensionless form $C_f/2C_h$ was chosen as a figure of merit to be used in comparing different geometries of both forced and natural draft heat exchangers. Heat exchanger configurations with low values of $C_f/2C_h$ have high performance with .7 being considered the minimum possible value when air is the fluid.

The first set of experiments were with a single row of circular tubes in a sawtooth pattern with half angles in the direction of flow of 15^o and 30^o and a spacing between tubes of 2.67 diameters. Values of $C_f/2C_h$ averaged 23 for angle of 30^o and 18 for 15^o with a Reynolds number based on tube diameter of about 10^4. Conventional heat exchangers made up of in-line arrangements of circular cylinders have $C_f/2C_h$ of 12 or less depending on the number of rows. Thus the sawtooth tube pattern does not appear to offer any advantage over conventional heat exchangers in terms of decreased pressure loss.

The second set of experiments was with a heat exchanger

of lenticular cross-sectioned tubes spaced so that the flow area between them was nearly constant (see figure). This had the effect of reducing the amount of separation in the flow and decreasing the value of $C_f/2C_h$.

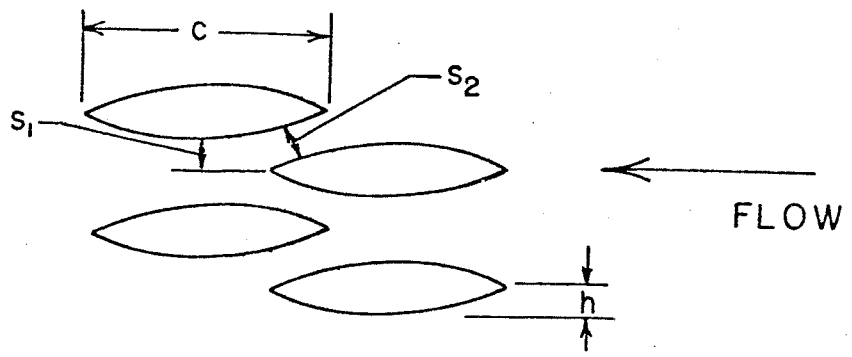

The ratio of chord to thickness of the tubes was 4 and the spacings were tested with 50, 66, and 78 percent of frontal area blocked. Tests were run with 3, 4, and 5 rows for each spacing. Most of the experiments were performed over a range of Reynolds numbers based on the chord of 50 to 75 000, Best performance was with 66% blockage and 5 rows which had an averaged value of $C_f/2C_h$ of 6.8. This is slightly superior to the performance of conventional in-line tube heat exchangers. Experiments were also performed for this spacing over a wider range of Reynolds number. Data from these experiments could be fit by the simple power curve $C_f/2C_h = .86\ (R_e)^{.185}$.

One problem that arose for some of the cases tested was the existence of a bubble of separated flow just downstream of the last

row in the tube array and centered on the top and bottom of the wind tunnel. This separation bubble resulted in decreased performance.

In conclusion it can be stated that the sawtooth tube pattern did not appear to offer any advantage over more conventional heat exchangers but the lenticular tubes were superior especially at the higher Reynolds numbers.

TABLE OF CONTENTS

I. INTRODUCTION

Interest in crossflow heat exchangers with low resistance to the flow normal to the axis of the tubes prompted this experiment to determine if certain unconventional shapes and arrangements of the heat exchanger might lead to a significant improvement in performance.

This investigation covered two different unusual configurations of cross flow heat exchangers. The first of these was an arrangement of circular cylinders in a sawtooth pattern. This was to test the persistent belief that this configuration was capable of achieving a high heat transfer rate with low drop in pressure. The second investigation concerned exchanger tubes of a special lenticular cross section so spaced as to keep the velocity of the fluid flowing outside the tubes nearly constant in magnitude, hence reducing adverse pressure gradients and hopefully lessening separation and drag.

The latter proved to be the more promising of the investigations and became the principal focus of attention.

II. REMARKS ON HEAT EXCHANGERS

Before considering the experiment a short discussion of the background is appropriate. Fluid flows across bundles of tubes with heat transfer, particularly tubes of circular cross section, have many important applications and have therefore been studied in considerable detail. Unfortunately the flow about such banks of tubes is too complex to be treated analytically and the available information is principally experimental. However an understanding of the important parameters is needed in order to interpret the experiments.

There are four basic arrangements of the two heat exchanger streams. These are shown schematically in figure 1. In parallel-flow heat exchangers two fluids of different temperature flow along the same axis in the same direction. In counterflow heat exchangers the fluids flow parallel to the same axis in opposite directions. The streams are normal to each other in the cross-flow type which can be either single-pass or multipass with one stream crossing back and forth through the path of the other flow. A stream may be mixed, flowing through a single passage, or unmixed in which it is broken up into many separate passages. One side can be mixed with the other unmixed or both sides may be the same. Also the two fluids are not necessarily the same, e.g. one may be liquid the other gas[1].

Each configuration has advantages in different applications. The major advantages of the cross flow heat exchanger over the others are that it can be made very compact, economizing on

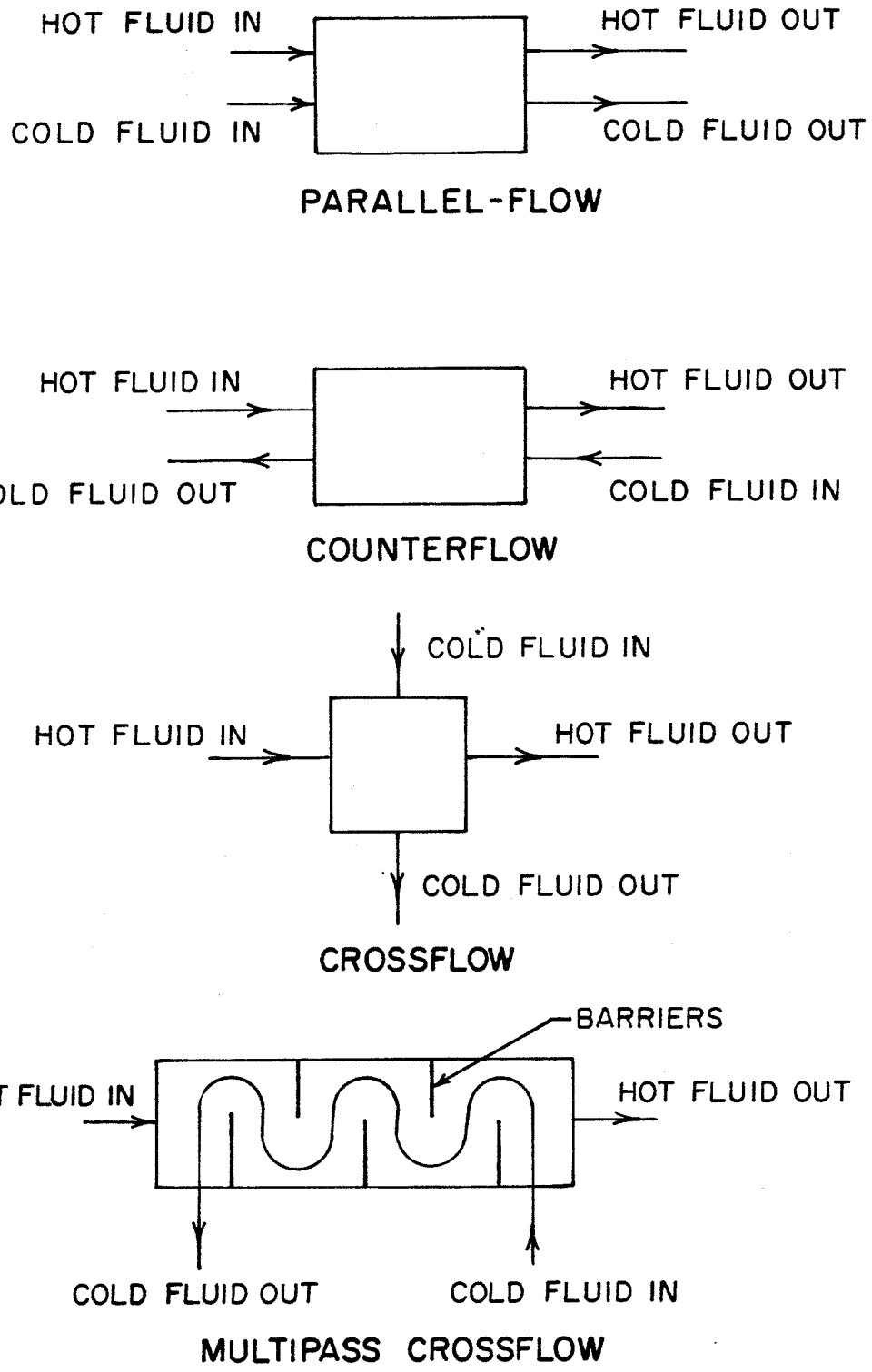

Figure 1. Heat Exchanger Basic Flow Path Arrangements

space and material, and that there is less difficulty in designing headers for two different streams. The major disadvantage is that in general they have a very large drop in pressure for the flow transverse to the tubes for a given heat transfer rate.

In some applications this pressure drop is of critical importance. Consider heat exchangers, such as in natural draft dry cooling towers, which depend on free convection to produce the flow. In such cases it is easy to see how a high drag can be detrimental to performance. Even with forced draft it is desirable to keep power consumption to a minimum, especially as energy costs rise. Thus there is an interest in crossflow heat exchangers that have high heat transfer with a minimum pressure loss.

Common types of crossflow heat exchangers, made up of either staggered or in-line arrangements of circular tubes, are shown in figures 2 and 3. These configurations are specified by the transverse spacing, s_t, the longitudinal spacing, s_ℓ, the tube diameter, d, and the number of rows, N.

The drag on the outside of a crossflow heat exchanger can be expressed as

$$A\Delta P = \frac{C_f}{2} \rho u^2 S. \tag{1}$$

The drag is equal to the frontal area of the heat exchanger, A, times the pressure difference across it, ΔP. $C_f/2$ is a dimensionless drag coefficient which would be the usual skin friction coefficient if there were no separation. ρ is the density of the

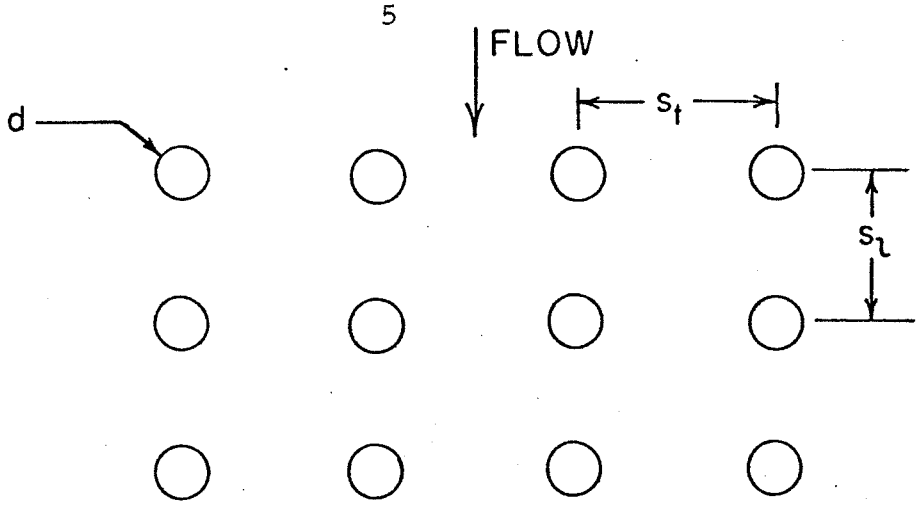

Figure 2. In-Line Cross Flow Heat Exchanger

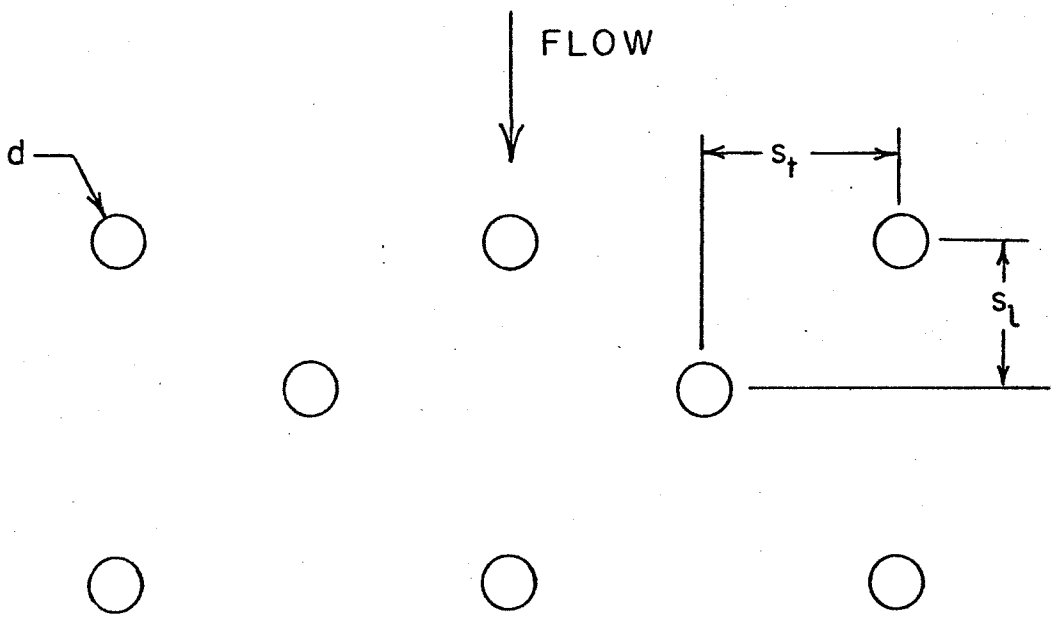

Figure 3. Staggered Cross Flow Heat Exchanger

fluid, u a reference velocity, and S the wetted surface area.

The heat flow rate, $\dot{Q}$, can be expressed as

2) $$\dot{Q} = \rho u c_p S \Delta T_w C_h$$

ρ, u, and S are the same as above. c_p is the specific heat at constant pressure for the fluid and ΔT_w is the temperature difference between the fluid and the wall of the heat exchanger. C_h is a dimensionless heat transfer coefficient known as the Stanton number.

The Stanton number is related to the usual convective heat transfer coefficient, h, by the equation

3) $$h = \rho u c_p C_h.$$

The local heat transfer rate per unit surface area is given by

$$\dot{q} = \frac{T_1 - T_g}{\frac{t}{k_w} + \frac{1}{h_1} + \frac{1}{h_g}}$$

where t is the wall thickness, k_w the thermal conductivity of the wall material, h_1 and h_g the heat transfer coefficients from liquid to wall and from wall to gas. The overall heat exchanger performance is determined by integration of $\dot{q}$ over the heat exchanger surface.

The pressure drop and heat transfer rates for flow inside tubes, even of non-circular cross section, is understood fairly well but the flow outside the tubes perpendicular to the tube axis is not well understood. In these experiments the wall conductivity

was high so the term t/k_w above could be neglected and instead of measuring the heat transfer from liquid to gas, the wall temperature was measured and attention concentrated on the gas side alone. In doing this it was assumed that the wall temperature was constant along the length of the tubes. Measurements indicated that the midpoint temperatures of the tubes were 70 to 90 C with a temperature drop of about 4 C across the length. The inlet air temperature was about 22 C so the assumption of constant wall temperature seems justified.

Reynolds[2] was the first to propose that heat and momentum should be transferred by similar processes in turbulent shear flow.

Suppose there is a turbulent shear layer with temperature gradient normal to flow direction. The heat flow rate per unit area, $\dot{Q}/S$, can be written

$$\frac{\dot{Q}}{S} = k_t \frac{dT}{dy}$$

where k_t is defined by this relation and could be considered a turbulent thermal conductivity, a property of the flow rather than a property of the medium. Similarly the effective drag per unit area can be written

$$\frac{A\Delta P}{S} = \mu_t \frac{du}{dy}$$

where μ_t is defined by this equation. Introduce a turbulent thermal diffusity defined as $\kappa_t \equiv \frac{k_t}{\rho c_p}$ and a turbulent momentum diffusity (kinematic viscosity) defined as $\nu_t \equiv \frac{\mu_t}{\rho}$. Then

$$\frac{\dfrac{A\Delta P}{S}}{\rho \dfrac{du}{dy}} \Big/ \frac{\dfrac{\dot{Q}}{S}}{\rho c_p \dfrac{dT}{dy}} = \frac{\nu_t}{K_t}$$

Reynolds made the assumption that in shear flow the turbulent transfer of momentum was a result of the same transport process as the turbulent transfer of heat. Hence $\nu_t \equiv K_t$ and u varies normal to the flow in the same way as T. Rewrite equation above as

$$\frac{\dfrac{A\Delta P}{S}}{\rho \bar{u} \dfrac{du}{dy}} \Big/ \frac{\dfrac{\dot{Q}}{S}}{\rho c_p \bar{u} \dfrac{dT}{dy}} = \frac{\nu_t}{K_t}$$

where $\bar{u}$ is the mean velocity. If $\nu_t = K_t$ throughout the flow even down to the wall then

$$\frac{\dfrac{du}{dy}}{\dfrac{dT}{dy}} = \frac{\dfrac{\bar{u}}{\Delta y}}{\dfrac{(T-T_w)}{\Delta y}} = \frac{\bar{u}}{(T-T_w)}$$

since u and T have similar shapes. Then from the definitions of C_f and C_h

$$\frac{C_f}{2C_h} = \frac{\nu_t}{K_t} .$$

We note that this relation holds only if $\nu_t = K_t$ right down

to the wall. Reynolds postulated that $\nu_t = \kappa_t$ in turbulent flow but if there is a laminar layer next to the wall then $C_f/2C_h = 1$ only if the Prandtl number $P_r \equiv \nu/\kappa = \mu c_p/k = 1$. For gases $P_r \approx 0.7$ so that we expect there would be little deviation from Reynolds analogy for gases in shear flow next to a wall.

In general the ratio of overall coefficients

$$\frac{C_f}{2C_h} = \text{fn } (P_r\ ,\ R_e\ ,\ \text{geometry})$$

where R_e is the Reynolds number. The Prandtl number appears because in the laminar flow region at the wall $\nu \neq \kappa$ in general; the Reynolds number appears because the ratio of thickness of laminar layer to overall boundary layer thickness is a function of Reynolds number.

The Reynolds analogy holds for turbulent flow of a gas for fluids inside a smooth tube and the value of $C_f/2C_h \approx 1$ appears to be lower than for any other configuration. Wall roughness or any other geometry that leads to flow separation increases drag more than heat transfer giving $C_f/2C_h > 1$.

The importance of $C_f/2C_h$ can be seen in another way. The pumping power, $\dot{W}$, required to drive the gas through the heat exchanger is given by the drag times the velocity.

$$\dot{W} = A\Delta P u$$

Thus the ratio of pumping power to heat flow rate is

$$\frac{\dot{W}}{\dot{Q}} = \frac{\frac{C_f}{2}\rho u^3 S}{\rho u c_p S \Delta T_w C_h} = \frac{C_f}{2C_h}\ \frac{u^2}{c_p \Delta T}\ .$$

For a forced draft application with a fixed velocity and temperature difference and a given heat flow rate the required pumping power will be a minimum for minimum $C_f/2C_h$.

The natural draft heat exchanger is slightly more complicated. Figure 4 is a schematic of natural draft heat transfer tower of height H. If the density outside the tower is ρ_o then the pressure drop outside is

$$P_o - P_2 = \rho_o \, g \, H \, .$$

The pressure drop inside the tower behind the heat exchanger where the density is ρ_1 is given by

$$P_1 - P_2 = \rho_1 \, g \, H \, .$$

The pressure drop across the heat exchanger is $P_o - P_1$ or

$$P_o - P_1 = (P_o - P_2) - (P_1 - P_2) = (\rho_o - \rho_1) \, g \, H \, .$$

Let

$$P_1 = P_o - \Delta P$$

and

$$T_1 = T_o + \Delta T$$

with

$$\frac{\Delta P}{P_o} << 1, \quad \frac{\Delta T}{T_o} << 1 \, .$$

Then

$$\rho_1 - \rho_o = \left(\frac{\rho_1}{\rho_o} - 1\right) \rho_o = \left(\frac{\frac{P_1}{RT_1}}{\frac{P_o}{RT_o}} - 1\right) \rho_o$$

$$= \left(\frac{P_1}{P_o} \frac{T_o}{T_1} - 1\right) \rho_o = \left[(1 - \frac{\Delta P}{P_o}) \, (\frac{T_o}{T_o + \Delta T}) - 1\right] \rho_o$$

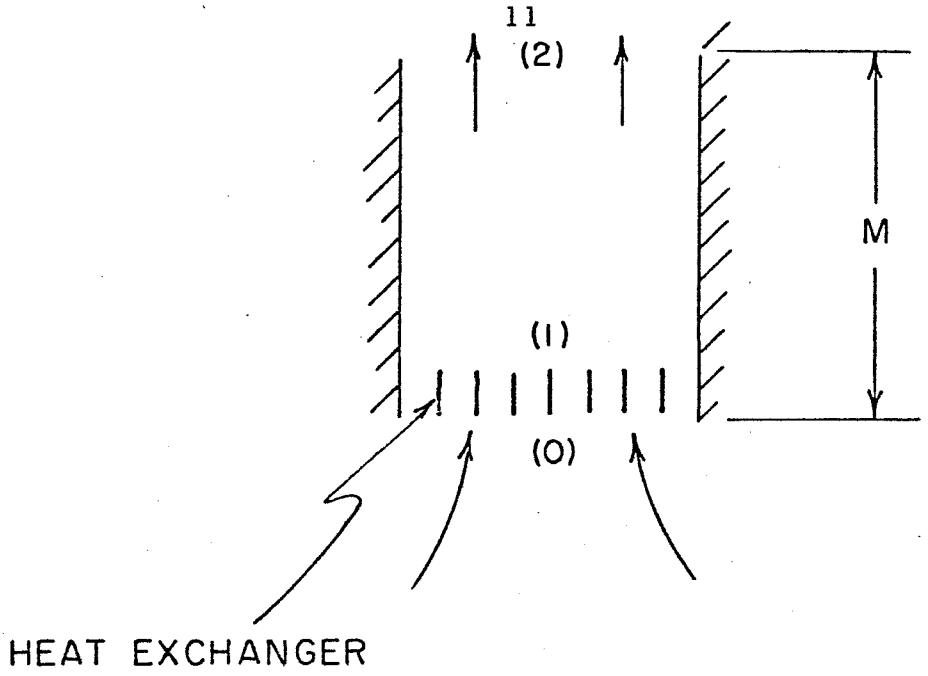

Figure 4. Natural Draft Heat Transfer Tower

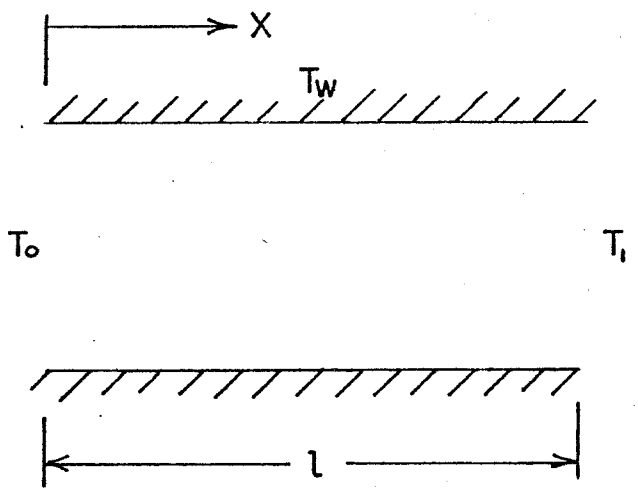

Figure 5. Heat Exchanger of Constant Wall Temperature

$$= \left[\left(1 + \frac{\Delta T}{T_o}\right)^{-1} - 1 \right] \rho_o$$

$$= - \frac{\Delta T}{T_o} \rho_o \ .$$

So

$$P_1 - P_o = - \Delta P = - \frac{\Delta T}{T_o} \rho_o g H$$

or

$$\Delta P = \rho_o g H \frac{\Delta T}{T_o} \ .$$

This pressure drop equals the pressure loss through the heat exchanger for low velocities

$$\rho_o g H \frac{\Delta T}{T_o} = \frac{C_f}{2} \rho u^2 \frac{S}{A} \ .$$

Next the heat flow rate is

$$\dot{Q} = c_p \rho u A \Delta T \ .$$

The temperature rise depends on the length, ℓ, of the heat exchanger. A multipass crossflow heat exchanger with constant wall temperature, T_w, is similar to the duct flow with constant T_w of figure 5. Here

$$A \rho u c_p \frac{dT}{d\xi} = C_h \rho u c_p S (T_w - T)$$

where $\xi \equiv \frac{x}{\ell}$. Let $\alpha \equiv C_h \frac{S}{A}$ then

$$\frac{dT}{d\xi} = \alpha (T_w - T)$$

or

$$T_w - T = A \, e^{-\alpha \xi} \ .$$

For $\xi = 0$ $T = T_o$ or $T_w - T_o = A$.

For $\xi = 1$ $T = T_1$ or $T_w - T_1 = A \, e^{-\alpha}$.

So

$$\frac{T_w - T_1}{T_w - T_o} = e^{-\alpha}$$

or

$$\frac{T_1 - T_o}{T_w - T_o} = 1 - e^{-\alpha} \equiv \epsilon .$$

So

$$\dot{Q} = c_p \rho u A \Delta T = c_p \rho u A \epsilon (T_w - T_o).$$

And

$$u = \frac{\frac{\dot{Q}}{A}}{c_p \rho \Delta T} = \frac{\frac{\dot{Q}}{A}}{c_p \rho \epsilon \Delta T_w} .$$

Then

$$\rho g H \epsilon \frac{\Delta T_w}{T_o} = \frac{C_f}{2} \rho \frac{S}{A} \left(\frac{\frac{\dot{Q}}{A}}{c_p \rho \epsilon \Delta T_w} \right)^2$$

so that

$$\frac{C_f}{2C_h} \frac{\frac{S}{A} C_h}{\epsilon^3} = \left(\frac{c_p}{R} P_o \right)^2 g H \left(\frac{\Delta T_w}{T_o} \right)^3 \left(\frac{\dot{Q}}{A} \right)^{-2}$$

or

$$\frac{C_f}{2C_h} \frac{\alpha}{(1-e^{-\alpha})^3} = \left(\frac{\gamma}{\gamma - 1} \right)^2 g H \left(\frac{\Delta T_w}{T_o} \right)^3 P_o^2 \left(\frac{\dot{Q}}{A} \right)^{-2}$$

since $\frac{c_p}{R} = \frac{\gamma}{\gamma - 1}$ where γ is the ratio of specific heats.

The expression $\frac{\alpha}{(1 - e^{-\alpha})^3}$ has a minimum for $\alpha = 1.9038$. The optimum value of $\frac{S}{A}$ is then $\frac{S}{A} = \frac{1.9038}{C_h}$.

Thus for the optimum $\frac{S}{A}$

$$\frac{\dot{Q}}{A} = .5690 \frac{\gamma}{\gamma - 1} \sqrt{g H} \left(\frac{\Delta T_w}{T_o} \right)^{\frac{3}{2}} P_o \left(\frac{C_f}{2C_h} \right)^{-2}$$

For a given ΔT_w, T_o, H, P_o, and configuration the heat transfer per unit frontal area is a maximum for the minimum value of $C_f/2C_h$.

The design of a heat exchanger is very dependent on the system of which it is a part. However, the parameter $C_f/2C_h$ would seem to have wide applicability as a figure of merit for comparison of heat exchangers of different geometries.

The sawtooth tube heat exchanger is shown in figure 6. This geometry is defined by the angle ϕ, the spacing s, and the diameter d. This investigation was limited to a single row of tubes.

The rather heuristic argument for preferring this form of heat exchanger is based on the assumption that the appropriate velocity to be used for determining pressure drop and heat transfer is the velocity normal to the tubes or the upstream velocity times sin ϕ. Recall from equation 1) that pressure loss goes as velocity squared but from equation 2) heat flow rate is proportional to just velocity. It has been suggested that by using this oblique tube arrangement the pressure drop will be reduced by $\sin^2 \phi$ while the heat flow rate by only sin ϕ as compared with the performance of a more conventional arrangement. The validity of these assumptions apparently has not been demonstrated experimentally and part of this investigation was directed toward testing them.

The lenticular tube heat exchanger is depicted in figure 7. The cross section of these tubes is two circle arcs joined together. Here the important parameters are the chord c, the half thick-

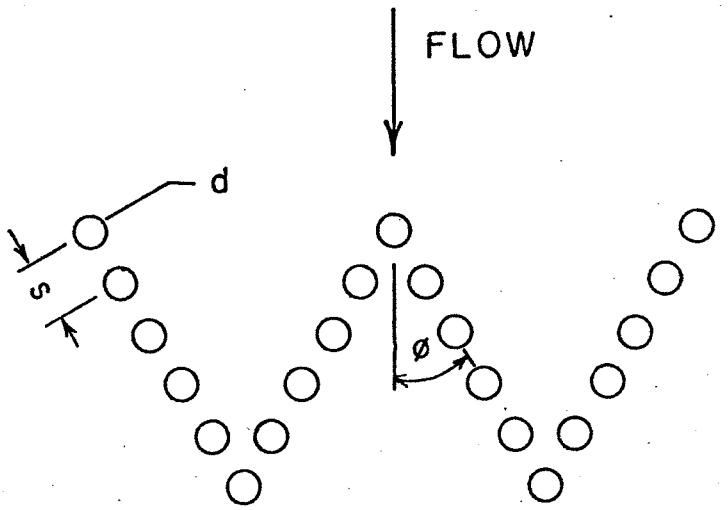

Figure 6. Sawtooth Heat Exchanger

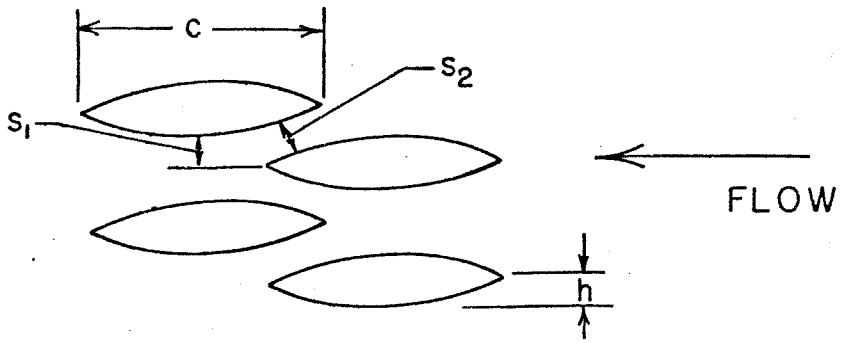

Figure 7. Lenticular Tube Heat Exchanger

ness h, the spacings s_1, s_2, and the number of rows N. The advantage of the lenticular shape is that by positioning the tubes appropriately the drag may be reduced. Aerodynamic drag on a body in subsonic flow is of two forms. The first results from friction on the surface of the body and is known as the skin-friction drag. The other type of drag is a result of separation of the flow in a region of adverse pressure gradient and subsequent failure of pressure recovery at the rear of the body. This type is called form drag. Very little can be done to reduce the skin-friction and low drag streamlined shapes are attempts to reduce the form drag by reducing the size of the separated regions. In the arrangements used here the spacing s_1 was set equal to s_2 thus making the flow area through the heat exchanger as nearly constant as possible. Then for incompressible flow the velocity is approximately constant with only modest accelerations and pressure gradients. This arrangement certainly produces smaller wakes and lower form drag for the tubes than is possible with tubes of circular cross section.

III. EXPERIMENTAL APPARATUS

A small, dedicated wind tunnel was built to carry out these experiments. The tunnel was made of 3/4 in. fir plywood and was about 20 ft. in length. It was an open-circuit tunnel with air drawn through it by a 7.5 hp. fan (see figures 8 and 9).

At the entrance to the tunnel there was a bell mouth followed by three closely spaced blocks of aluminum honeycomb each 5 in. thick with a 1/16 in. cell size. Besides straightening and helping to smooth out the incoming flow these honeycomb blocks acted as a thermal capacitor to reduce any rapid temperature fluctuations of the entering flow that might affect temperature measurements. The theory of the thermal mass is given in appendix A. We have estimated that temperature fluctuations of frequencies greater than .25 Hz are reduced to less than 1% of original amplitude. Unfortunately the thermal mass does not help with non-uniformity of temperature over inlet cross section. The honeycomb was made of very thin foil so thermal conduction through the solid material normal to the flow was negligible. Non-uniform inlet conditions may result from sources of hot or cold air too near the tunnel entrance. For example, placement of a hot water tank 6 ft. behind the tunnel entrance resulted in a non-uniform temperature distribution in the test section and the tank had to be moved farther away.

The entire test section could be removed easily and replaced by another test section. In addition panels forming part of the upper and lower walls of the test section could be readily removed

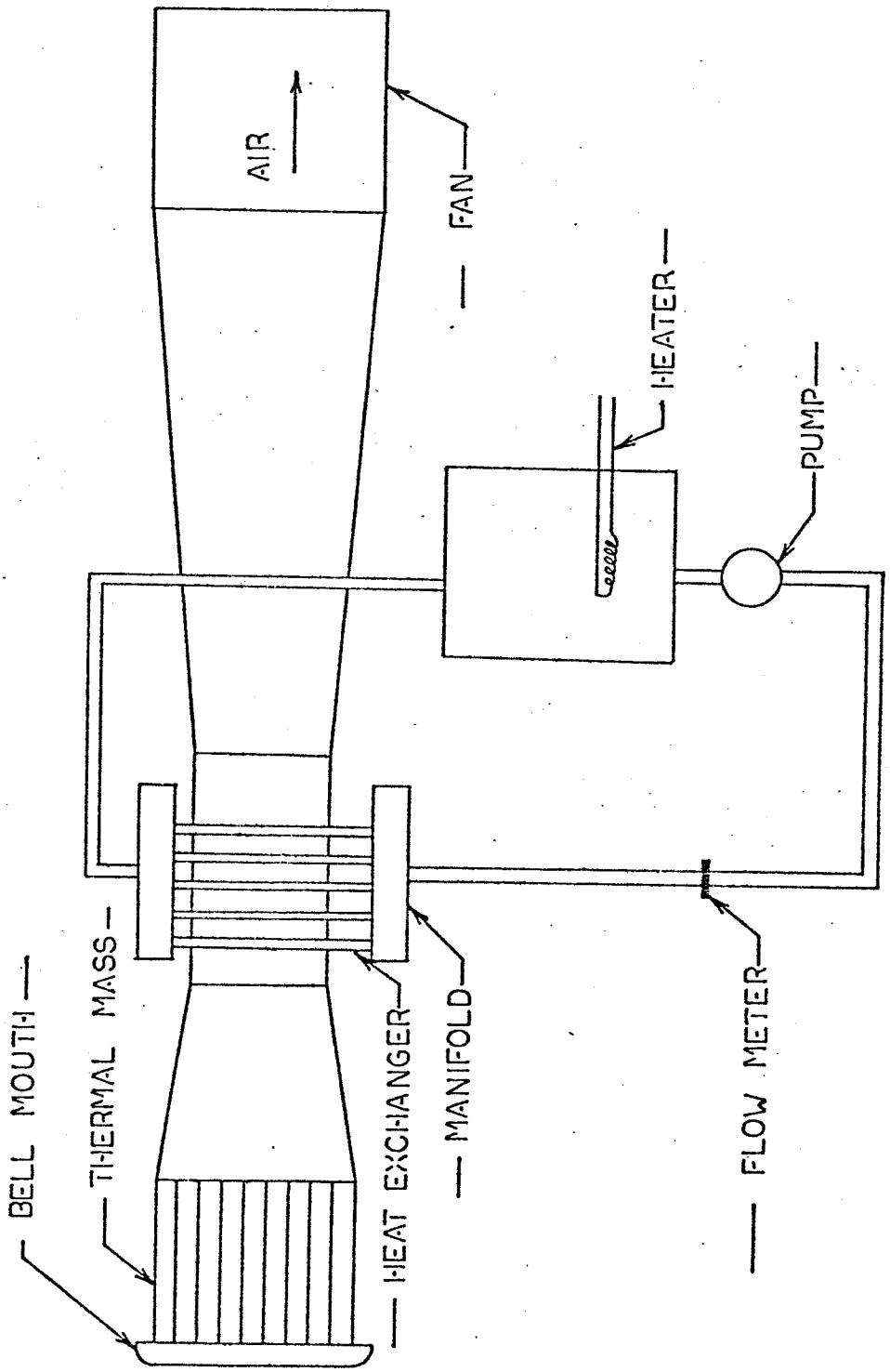

Figure 8. Wind Tunnel Layout

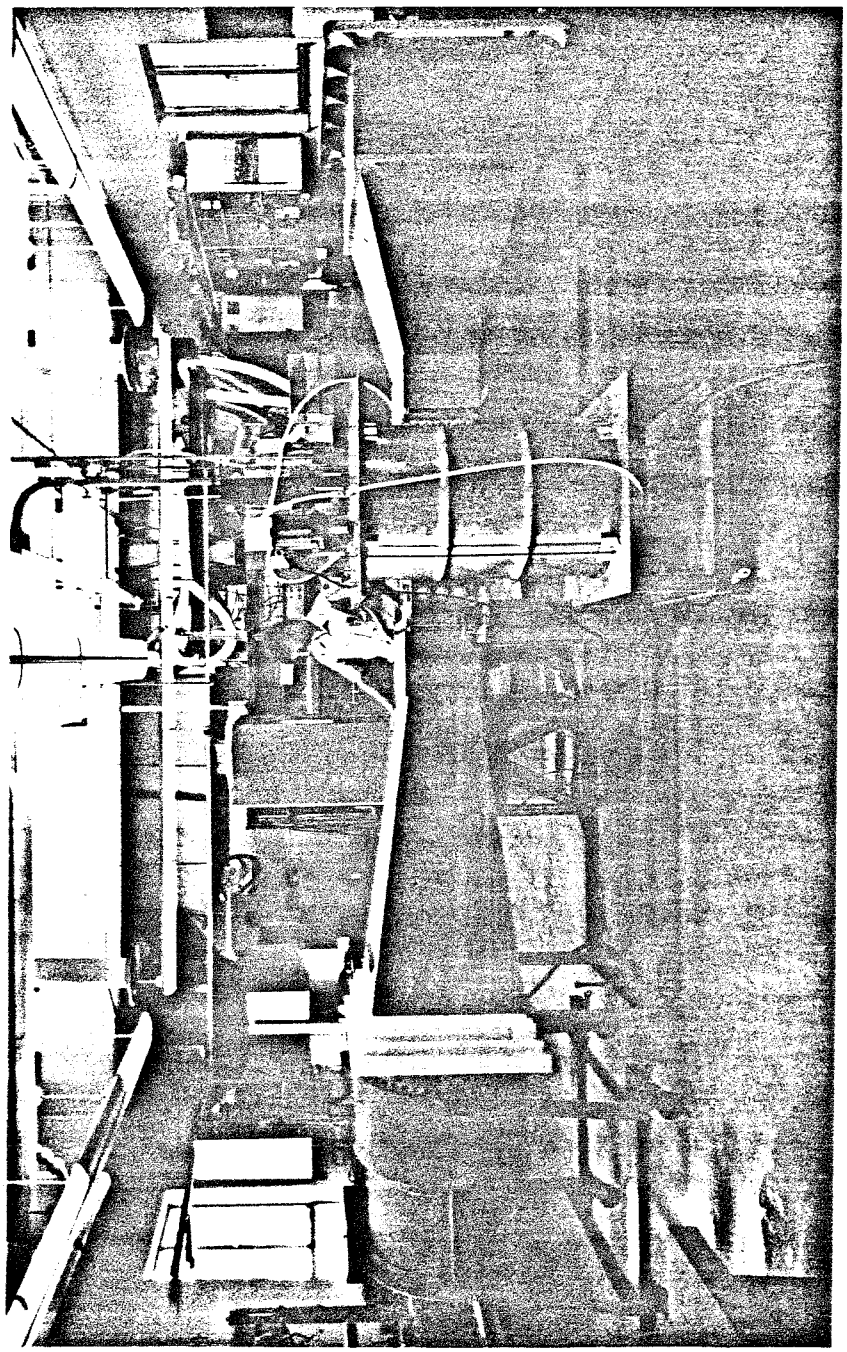

Figure 9. Wind Tunnel Photo

and replaced by others for different heat exchanger configurations. The heat exchanger consisted of metal tubes inserted through holes cut in these panels. The working section was 9 in. high and 16 in. wide (1 ft.^{2} in area). The maximum velocity through the empty tunnel was about 25 m/s.

In operation, water was heated to a temperature of 70 to 99 C (depending on the application) in a 55 gal. stainless steel drum by a 5kW electric resistance heater and was thoroughly stirred before being pumped upward into a manifold which distributed the hot water through flexible hoses to the heat exchanger tubes. After passing through the working section the water was collected by an upper manifold and returned to the heater tank to be recycled. There are 22 ports on each manifold allowing a maximum of 22 heated tubes.

The water mass flow rate was determined by an orifice flow meter located 3 in. upstream of the first manifold. The manifold inlet had a 1.0 in. ID and the orifice diameter was .5 in. The pressure difference across the orifice was read with a water manometer. The pressure taps were .5 in. downstream and 1.0 in. upstream of the orifice. The system was calibrated in place.

Iron-constantan thermocouples made of .005 in. diameter wire were packed with silicone grease, mounted into brass tubes 1/16 in. in diameter, and inserted into both manifolds with one located 11.5 in. upstream of the first manifold and one 1.5 downstream of the second manifold. When referenced against each other these thermocouples measure the temperature drop

in the water as it flows through the manifolds, connecting plastic tubes and heat exchanger tubes.

Similar thermocouples were laid into shallow grooves cut along the length of the heat exchanger tubes with their junctions at the midpoint and referenced to a total temperature probe upstream of the tube bank. These gave the difference between the tube wall temperature and the temperature of the undisturbed air. On the sawtooth tubes the slot was at the forward stagnation point, in the lenticular tubes at the 1/2 chord.

All thermocouple outputs were measured on a Keithley Model 174 digital multimeter capable of reading voltages to .1 μV (corresponding to a temperature resolution of .03 K.). Where necessary the thermocouple wires were wound together to reduce spurious signals from fluctuating magnetic fields in the room.

The static pressure drop across the heat exchanger was found by referencing 3 upstream static pressure taps in the floor of the tunnel against 3 downstream static pressure taps and averaging these readings together. The pressures were measured by means of a Datametrics 538-10 Barocel pressure sensor and a Type 1014A electronic manometer.

Because the fan runs at constant speed the flow rate through the test section was varied by opening or closing bypass ports in front of the fan. The test section velocity could be changed by a maximum of 23% in this way. When larger reductions in flow velocity were needed the fan exit was partially blocked. The velocity was determined by a calibration of the upstream pressure

taps referenced to atmosphere. A pitot probe placed in the empty test section was used for calibration.

There were also provisions for inserting a total temperature probe and a pitot probe into the tunnel at a number of locations upstream and downstream of the heat exchanger.

The tubes in the sawtooth heat exchanger were made of 3/8 in. O.D. stainless steel tubing with a .046 in. thick wall (see figure 10). Since the manifold had provision for only 22 tubes the middle tubes alone could be "active" with hot water flowing through them. The rest were unheated, "passive" tubes. This was felt to be an acceptable procedure as long as the temperature profile had a steep gradient downstream of the boundary between active and passive tubes. The wetted surface of all the tubes was used for the calculation of $C_f/2$ and the surface area of the heated tubes alone for C_h.

The lenticular tubes were constructed by cutting segments from a 4 1/4 in. O.D. brass pipe, milling the edges flat, and soldering two pieces together. The chord was 2 in., the half thickness was 1/4 in., and the wall was 1/8 in. thick. Since these tubes were expensive to manufacture, only the active tubes were made of metal. The passive tubes were made by mounting 1/4 in. pieces of pine onto a 4 x 4 in. aluminum block and turning them to the correct radius on the lathe. Two of these pieces were then glued together to make up a passive tube. (See figure 11)

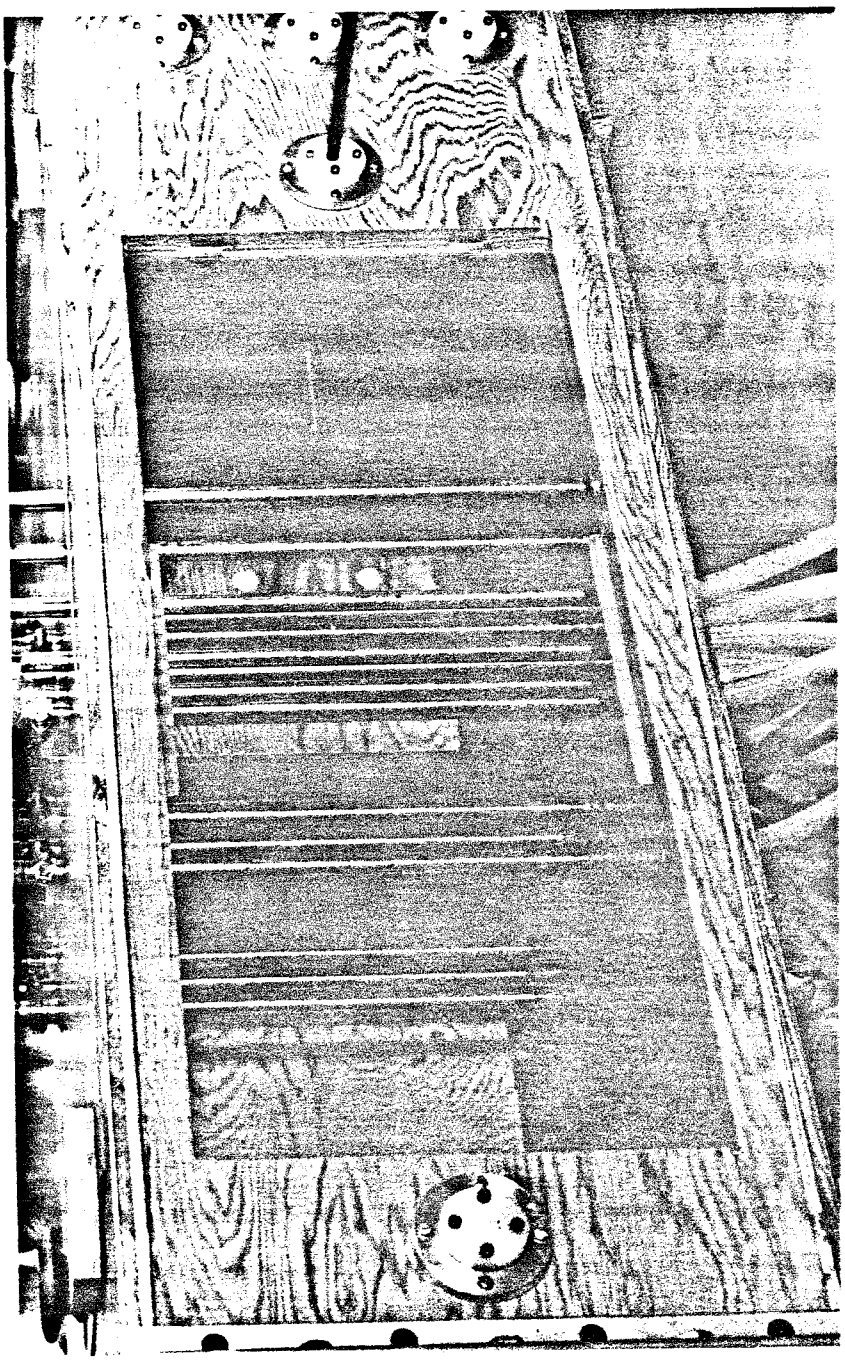

Figure 10. Test Section With Sawtooth Tubes

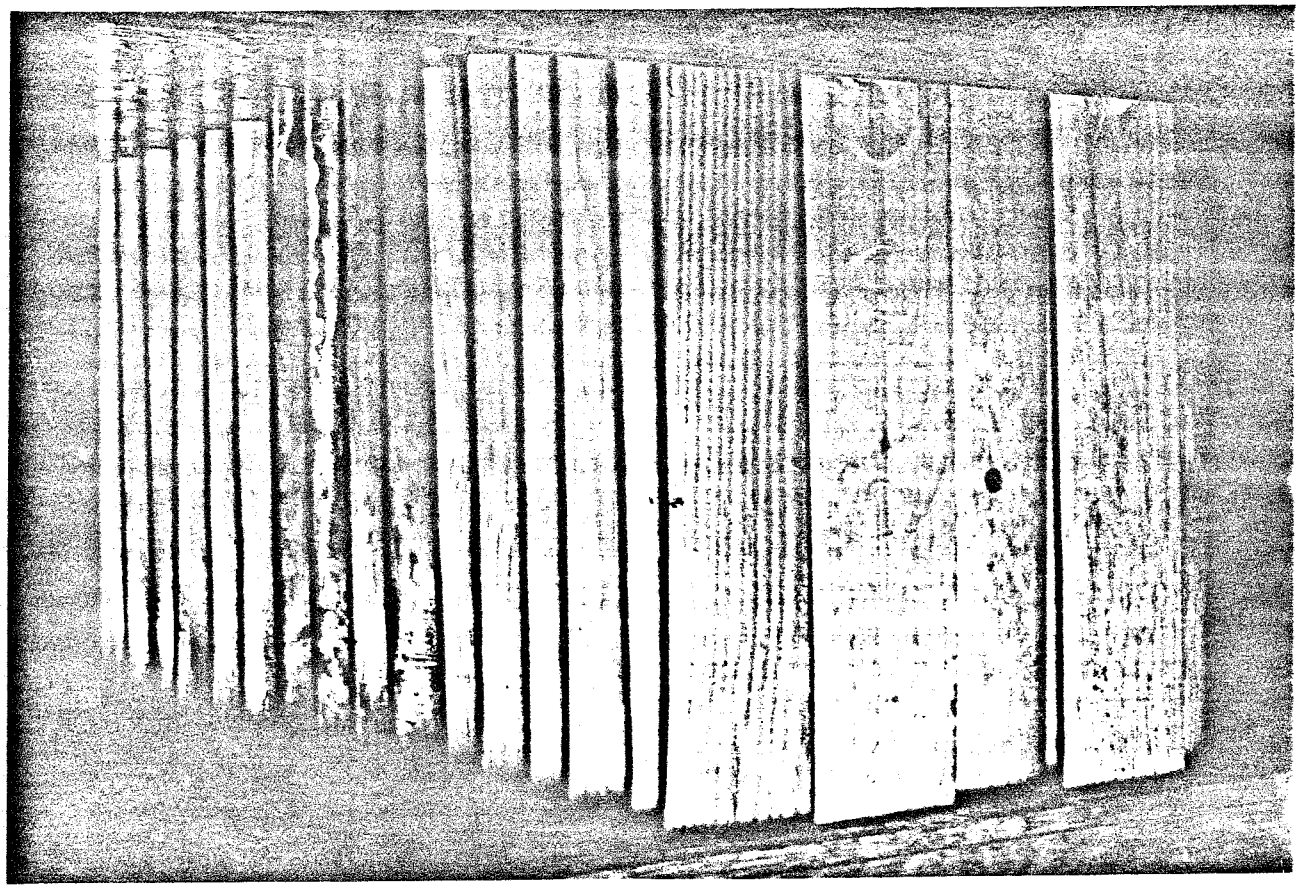

Figure 11. Test Section With Lenticular Tubes

IV. EXPERIMENTAL PROCEDURE

A typical test of a configuration involved operating the system until the heated water in the tank reached an equilibrium temperature. At this point the following quantities were measured: the water temperature drop across the heat exchanger, ΔT_{H_2O}; the temperature difference between a reference point on the tube wall and the undisturbed air, ΔT; the averaged pressure loss across the heat exchanger, ΔP; and the upstream velocity, u_∞

The heat flow rate is

$$\dot{Q} = c_{p_{H_2O}} \dot{m}_{H_2O} \Delta T_{H_2O}$$

where $c_{p_{H_2O}}$ is the water specific heat at constant pressure and is assumed to be constant over the range of water temperature used in the test. The Stanton number from 2) is then:

$$C_h = \frac{c_{p_{H_2O}}}{c_p} \frac{\dot{m}_{H_2O}}{\rho u S_{heated}} \frac{\Delta T_{H_2O}}{\Delta T}$$

In some cases u was taken as u_∞ in others the Stanton number was based on the nominal maximum velocity through the tube bank u_{max}. The particular reference velocity used will be discussed later. S_{heated} is the surface area of the heated tubes.

The pressure loss coefficient is found from 1)

$$\frac{C_f}{2} = \frac{\Delta P}{\rho u^2} \frac{A}{S}$$

Where u is the same as the velocity used in the previous equation for Stanton number and S is the total wetted area of the heat exchanger.

The tunnel velocity was altered to vary the Reynolds number and the test repeated.

In addition to the measurements above velocity and temperature surveys were also made for each case. Integrating results from these surveys gave checks on the heat and mass flow rates. The air mass flow rate is:

$$\dot{m}_{air} = \int_0^H \int_0^W \rho u(x)\, dx\, dy.$$

H and W are the height and width of the tunnel. u(x) is the velocity profile.

The heat flow rate from the temperature profile is:

$$\dot{Q} = c_p \int_0^H \int_0^W \rho\, u\, (x)\, \Delta T(x)\, dx\, dy.$$

For sufficiently thin wall boundary layers at the tube ends and ignoring the small density change these expressions can be written:

$$\dot{m}_{air} = H\rho \int_0^W u(x)\, dx$$

$$\dot{Q} = H\rho c_p \int_0^W u(x)\, \Delta T(x)\, dx.$$

In the early test we assumed that the upstream temperature, T_∞, was constant and could be read from an accurate thermometer near the tunnel inlet and did a survey only for the downstream temperature profile T(x) so that

$$\Delta T(x) = T(x) - T_\infty$$

It was found that because of the small difference between T(x) and T_∞ that some precision was lost in subtracting them to

find $\Delta T(x)$. To improve on this two temperature probes were referenced against each other to give $\Delta T(x)$ directly. Also the upstream probe was moved to keep it aligned with the quarter of the test section being traversed by the downstream probe to account for possible variation in T_∞ across the width of the test section.

These surveys were made along the tunnel midplane and they did not include the boundary layers on the upper and lower tunnel surfaces. The boundary layers downstream of the lenticular tube heat exchanger were not small and caused some discrepancy between the integrated heat and mass flow ratio and those determined more directly. Generally the mass flow rate was 10% higher and the heat flow rate 5% lower for the integrated measurements than for the direct measurements. These discrepancies can be explained by the facts that the flow rate is retarded in the boundary layers causing the midplane velocities to be higher and that vertical temperature surveys showed the temperature and hence heat flow rates to be higher in the boundary layers than in the midplane. The direct measurements are presumed to be more accurate with the less elaborate integrations serving as a check.

V. SAWTOOTH HEAT EXCHANGER

Two different patterns of sawtooth heat exchanger tubes were tested. One with $\phi = 30^{\circ}$ and $s/d = 2.67$; the other had $\phi = 15^{\circ}$ and $s/d = 2.67$.

ΔT was based on a thermocouple mounted at the forward stagnation midpoint of the tube in the center of the tunnel referenced to an upstream probe. The reference velocity used was u_{∞} and the Reynolds number was based on this velocity and the tube diameter

$$R_e = \frac{u_{\infty} d}{\nu}$$

ν is the kinematic viscosity of air.

Figures 12 and 13 show the temperature and velocity profiles along the centerline of the tunnel 9.5 diameters downstream of the array for $\phi = 30^{\circ}$ and the tunnel running at full speed. Figure 12 clearly shows a sharp rise in the temperature profile across the boundary between active and passive tubes with a rather flat profile across the width of the heated tubes. The velocity distribution reflects the sawtooth tube pattern, the valleys being caused by the wakes of the tubes nearest the pitot probe.

Figure 14 is a plot of $C_f/2$ vs. R_e for $\phi = 15^{\circ}$ and 30°. There is little variation in $C_f/2$ for the two cases over the limited range in Reynolds number tested. Clearly the configuration with $\phi = 15^{\circ}$ has less drag. The Stanton number is plotted in figure 15 which shows the heat transfer is the same for both cases. The ratio of $C_f/2C_h$ plotted against R_e is shown in figure 16. Because of its lower drag, performance is somewhat better for $\phi = 15^{\circ}$,

but neither arrangement is near the Reynolds analogy.

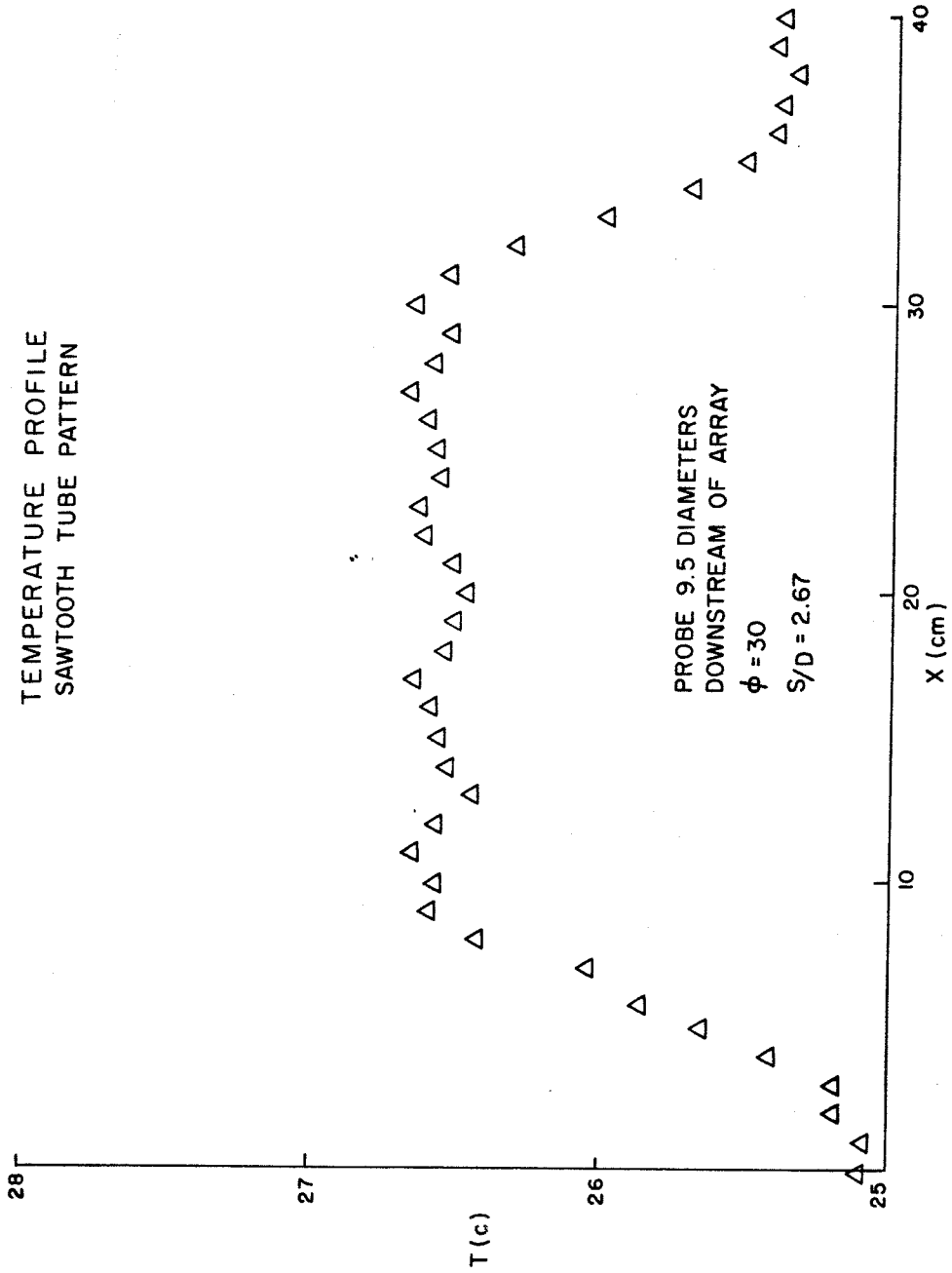

Figure 12. Temperature Profile Sawtooth Tubes

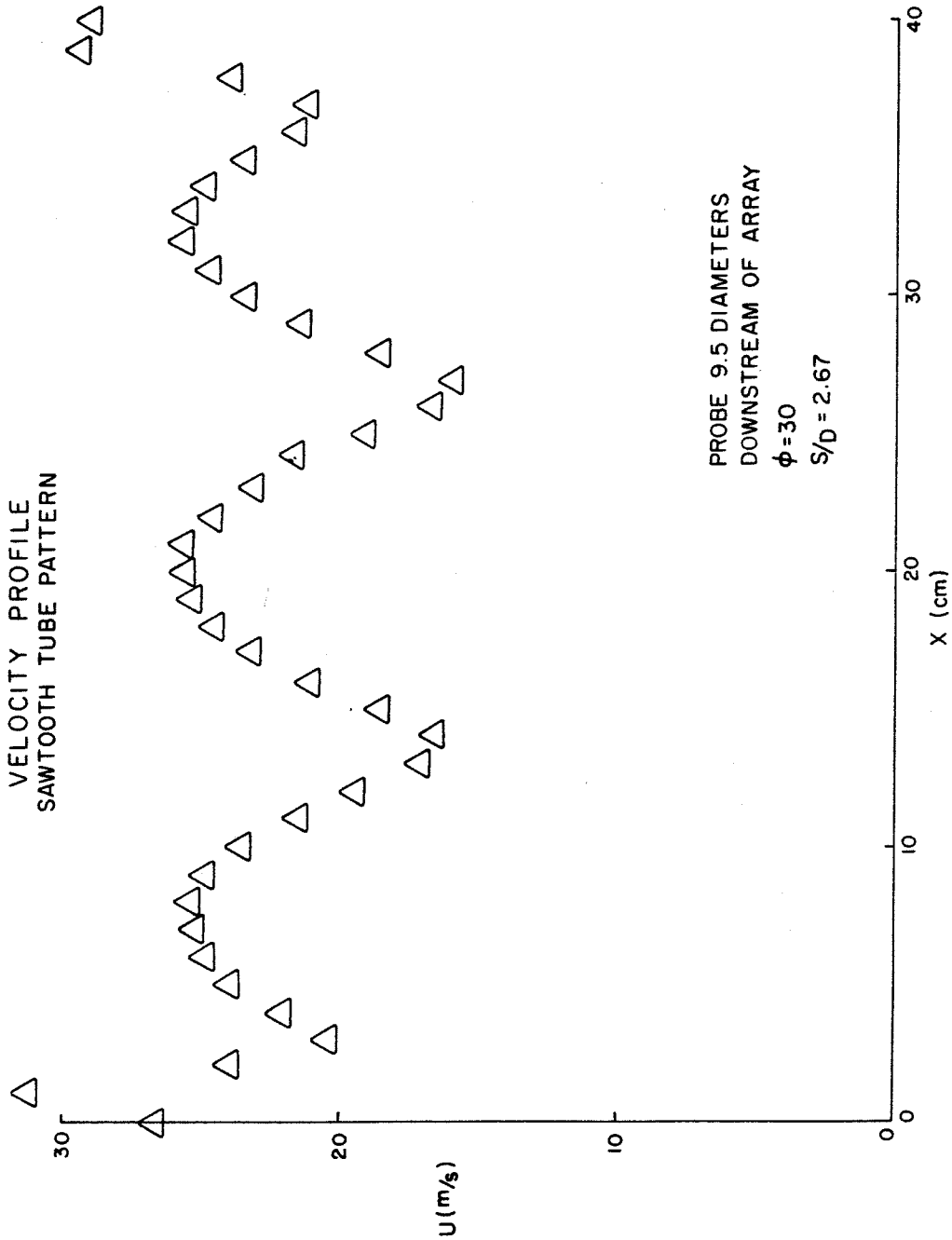

Figure 13. Velocity Profile Sawtooth Tubes

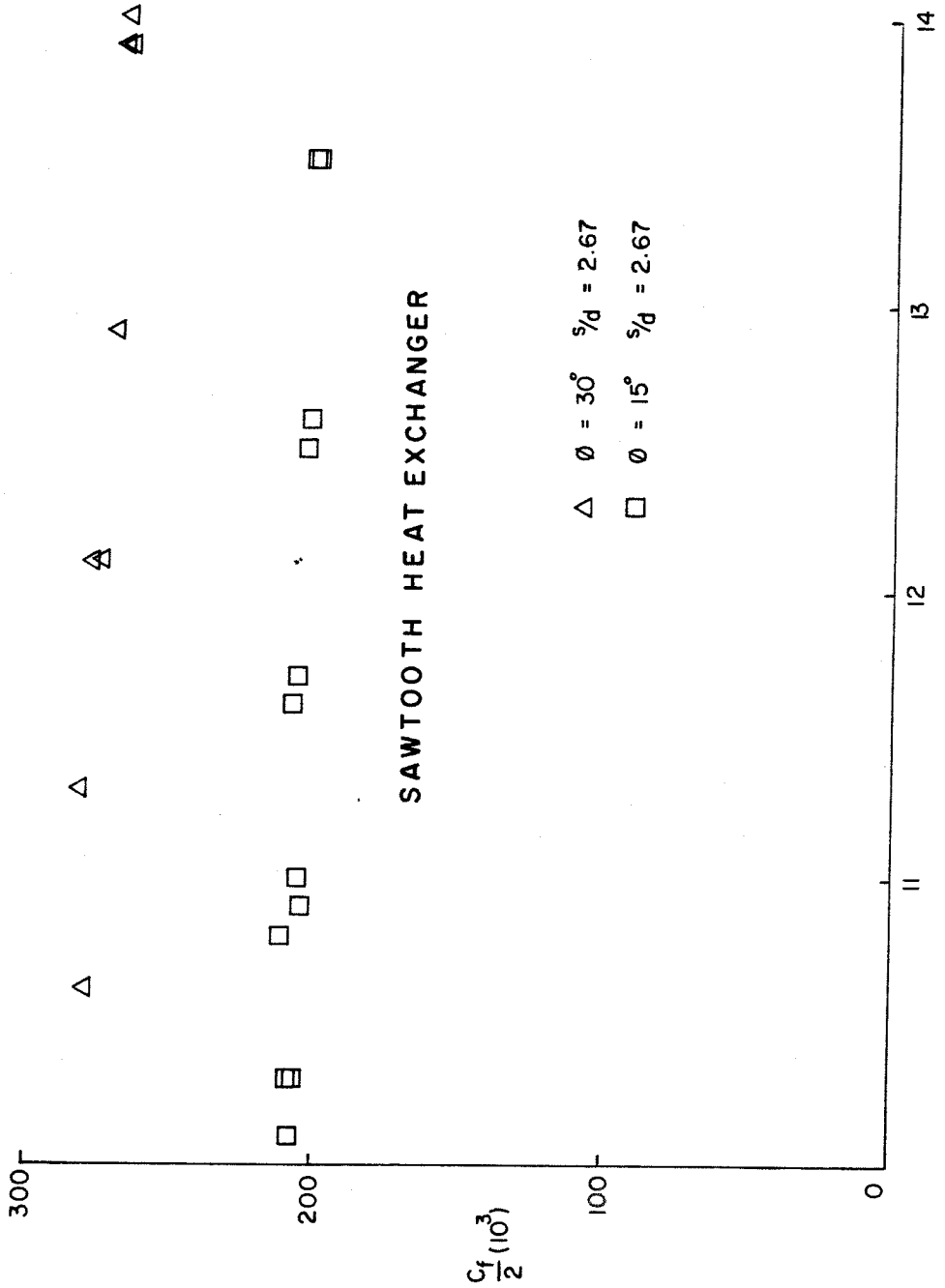

Figure 14. $C_f/2$ vs. R_e Sawtooth Tubes

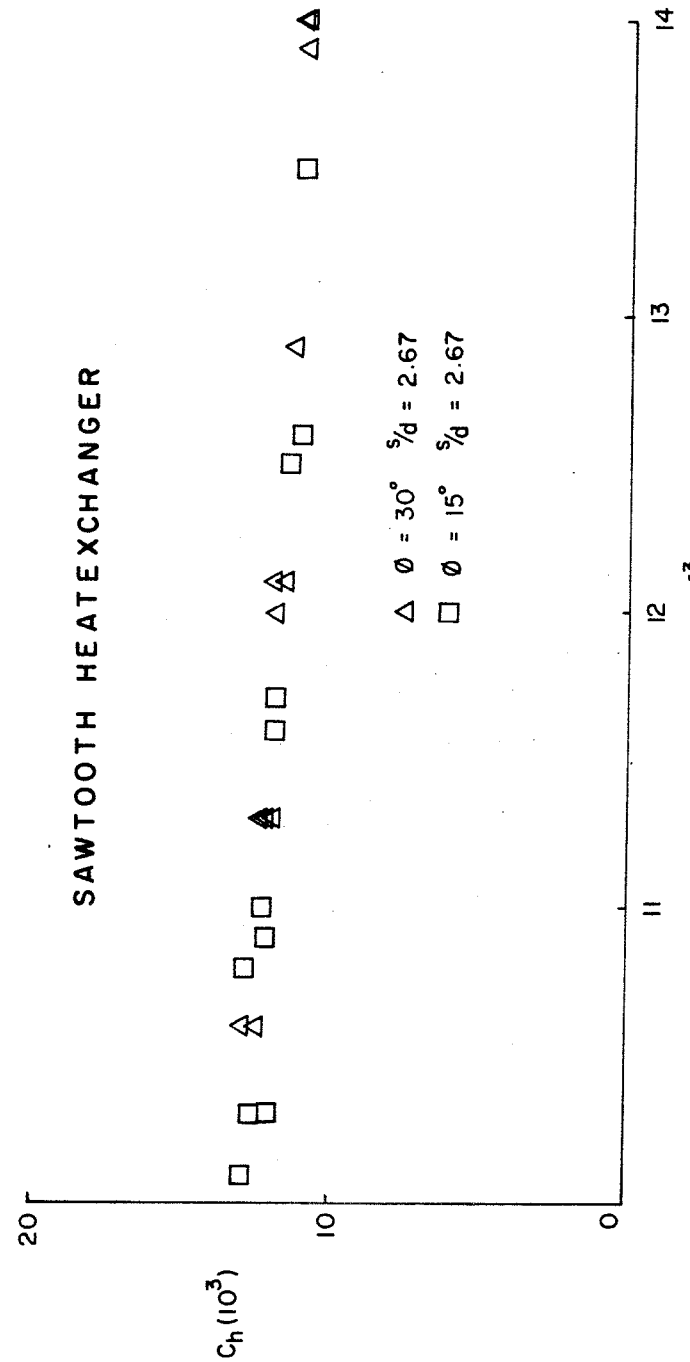

Figure 15. C_h vs. R_e Sawtooth Tubes

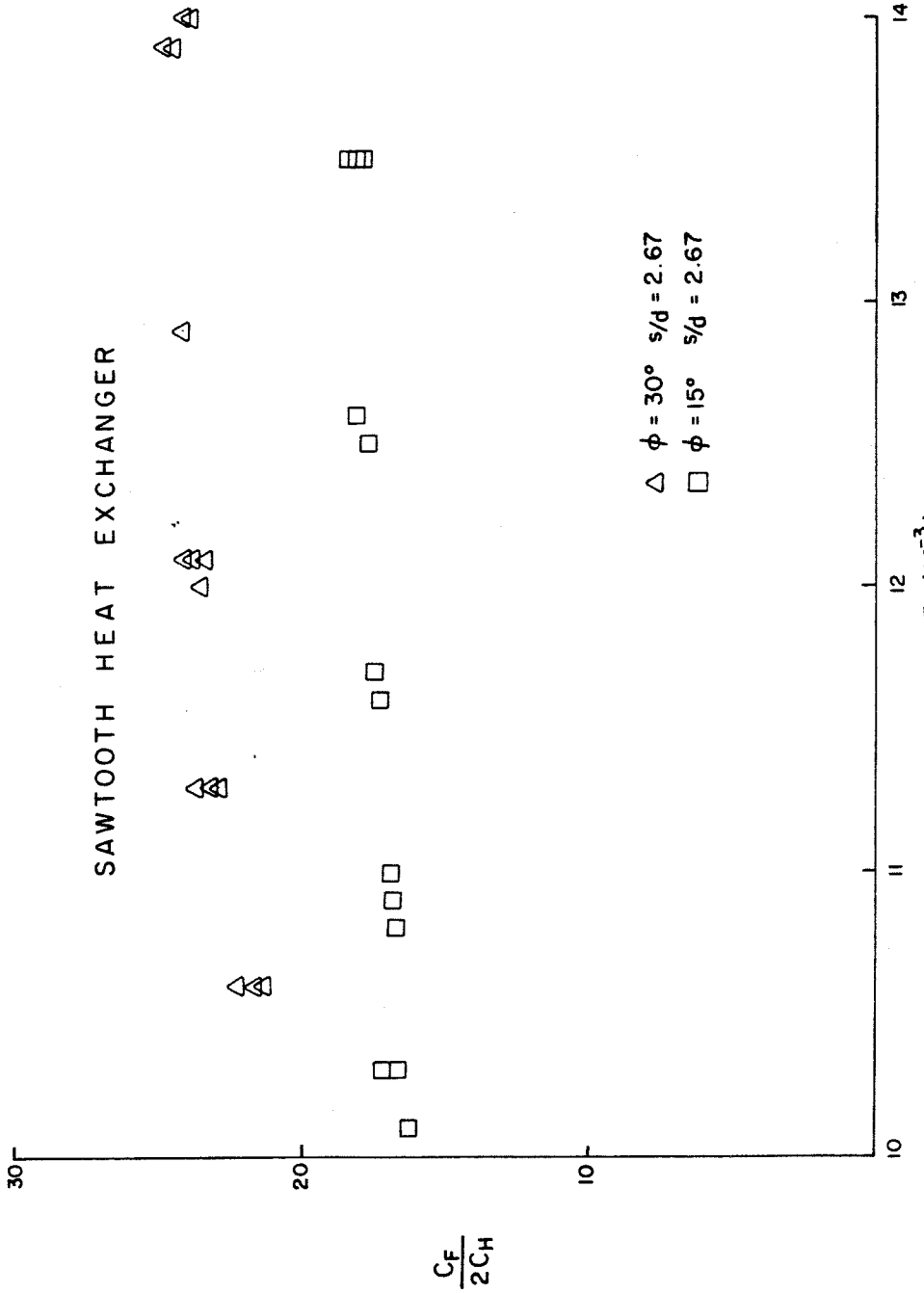

Figure 16. $C_f/2C_h$ vs. R_e Sawtooth Tubes

VI. LENTICULAR TUBE HEAT EXCHANGER

Three spacings of lenticular tubes were investigated: $s_1/h = s_2/h = 1.00$, $s_1/h = s_2/h = 3.50$, and the geometric mean of the two $s_1/h = s_2/h = 1.91$. Tests were run with 3, 4 and 5 rows for each case.

For the lenticular tubes it was discovered that heat losses through exposed tubing and the manifolds were greater than expected. These losses were about 20% of the total heat flow rate. They were measured by insulating the heat exchanger and measuring the heat flow rate for the rest of the system as a function of water temperature. This tare was then subtracted from the overall heat loss to obtain the heat flow through the heat exchanger.

For $s_1 = s_2 = h$ there were discrepancies in the velocity surveys made far downstream of the tube bank. The profile was non-uniform with large velocity defects. To find out what was happening, tufts were placed along the roof and floor of the test section. These showed there was a region of recirculating flow on the end walls at the center of the tunnel and that it was some 10 to 15 cm. wide. A vertical total pressure probe was made by drilling a number 80 hole into a 1/16 O.D. tube. Vertical surveys indicated that the height of the separation bubble was from 1 to 2 cm. Moving the probe forward inside the tube array indicated that the separation did not extend far upstream into the tube bank.

The general appearance of the separation bubble is shown in figure 17.

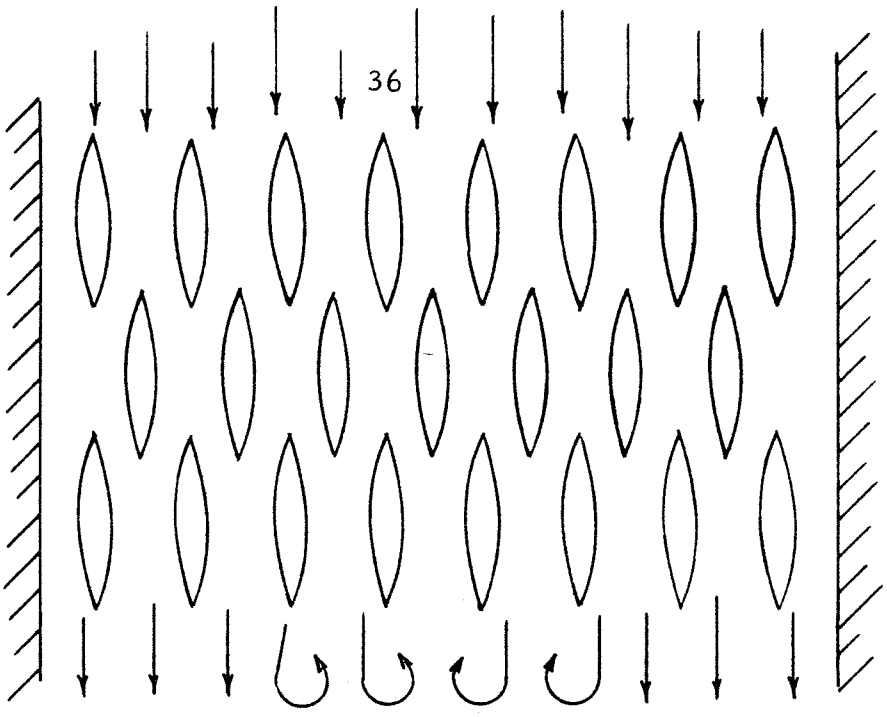

TOP VIEW

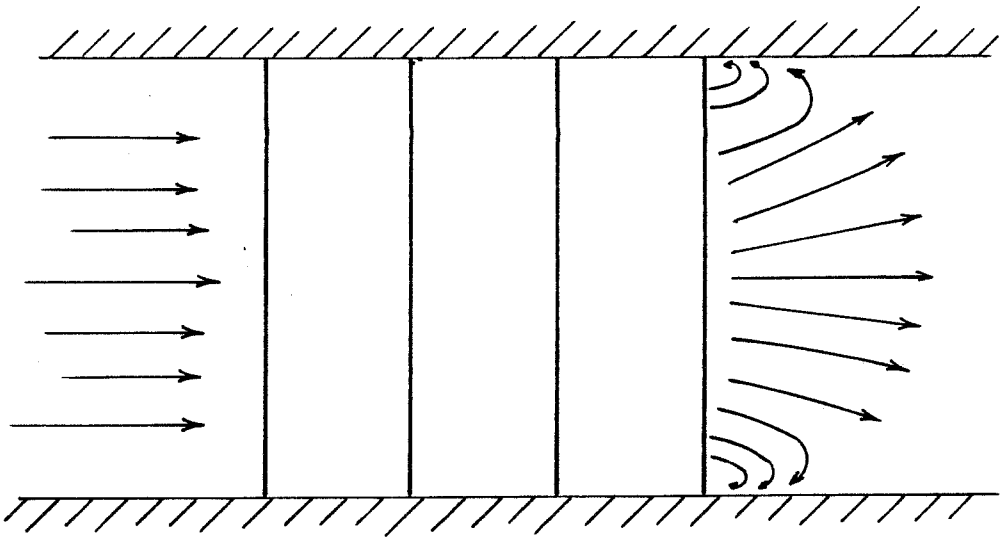

SIDE VIEW

Figure 17. Separation Bubble

The large variations in the velocity profile far downstream apparently were caused by the rolling up of vortices from the separated region. Measurements close to the last row were much easier to interpret than those far downstream.

It appears that the boundary layer builds up along the corners of the tunnel surfaces and the outer tube walls. At the last row the cross sectional area of the channels between the tubes diverges rapidly and the consequent deceleration, if large enough, tends to cause separation of the flow from the tube walls. In effect this last row of tubes forms an array of diffusers. The closer the tube spacing the greater the diffuser angle. Why this occurs only in the center of the top and bottom walls of the tunnel instead of across the whole test section width is not clear, but seems to have something to do with the presence of the tunnel side walls. An analogy might be made with the case of a stalled three dimensional wing where separation occurs in patches relieving conditions along the rest of the wing where the flow remains attached.

The separation problem existed for many of the arrangements and had a noticeable effect on performance as will be discussed later.

Figure 18 shows the effect on $C_f/2C_h$ of the different spacings with 3 rows. The reference velocity is u_∞ and the Reynolds number is based upon the tube chord.

Tufts indicated that there was separation for $s_1/h = s_2/h = 1$ but not for the other two cases. The figure is interpreted as

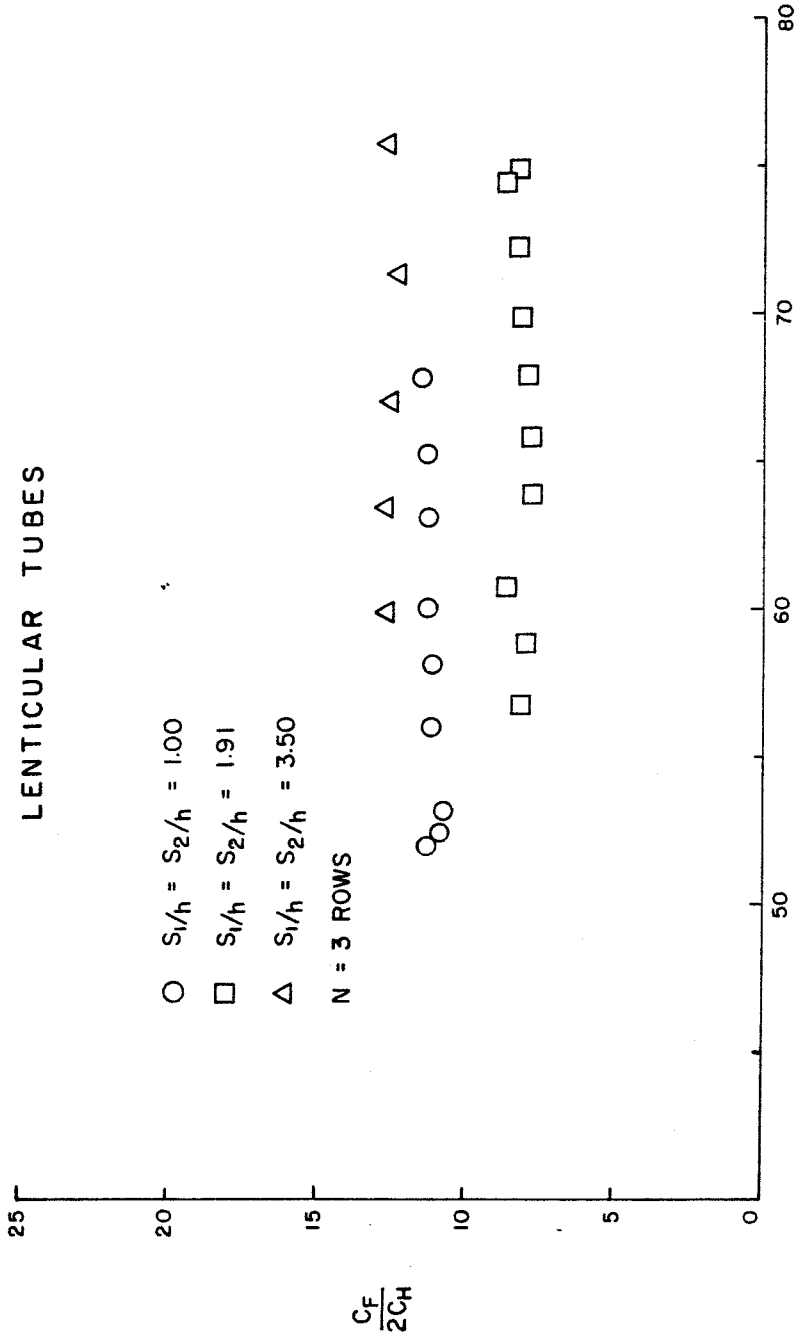

Figure 18. $C_f/2C_h$ vs. R_e N = 3 Lenticular Tubes

indicating that the tube arrangement reduces the form drag for the closely spaced case $s_1 = s_2 = 1$ h through the heat exchanger but the separation bubble that exists after the last row somewhat decreases performance.

For the wide spacing $s_1 = s_2 = 3.5$ h no separated region was observed but the tubes are too far apart for the spacing to be effective in reducing form drag, the situation must be like flow about individual tubes rather than through a bank of tubes with uniform separation over the cross section rather than in patches. Thus these two spacings are very close in performance for different reasons.

For $s_1 = s_2 = 1.91$ h the tubes are closer together so that the diffuser angle is less allowing the flow to remain attached. Performance was superior for this case.

With 4 rows the relative positions of the three spacings have not changed but overall performance has improved as shown in figure 19. Again, only the configuration with $s_1 = s_2 = 1$ h has the separated region.

The situation changed with 5 rows as is shown in figure 20. Here the arrangement with $s_1 = s_2 = 1.91$ h also led to a separated region so that all three spacings are close together in performance.

Next we examine each spacing individually. The reference velocity in the figures that follow is based on the nominal maximum velocity in the interior of the heat exchanger, that is, the velocity through the minimum area. The Reynolds number is based upon

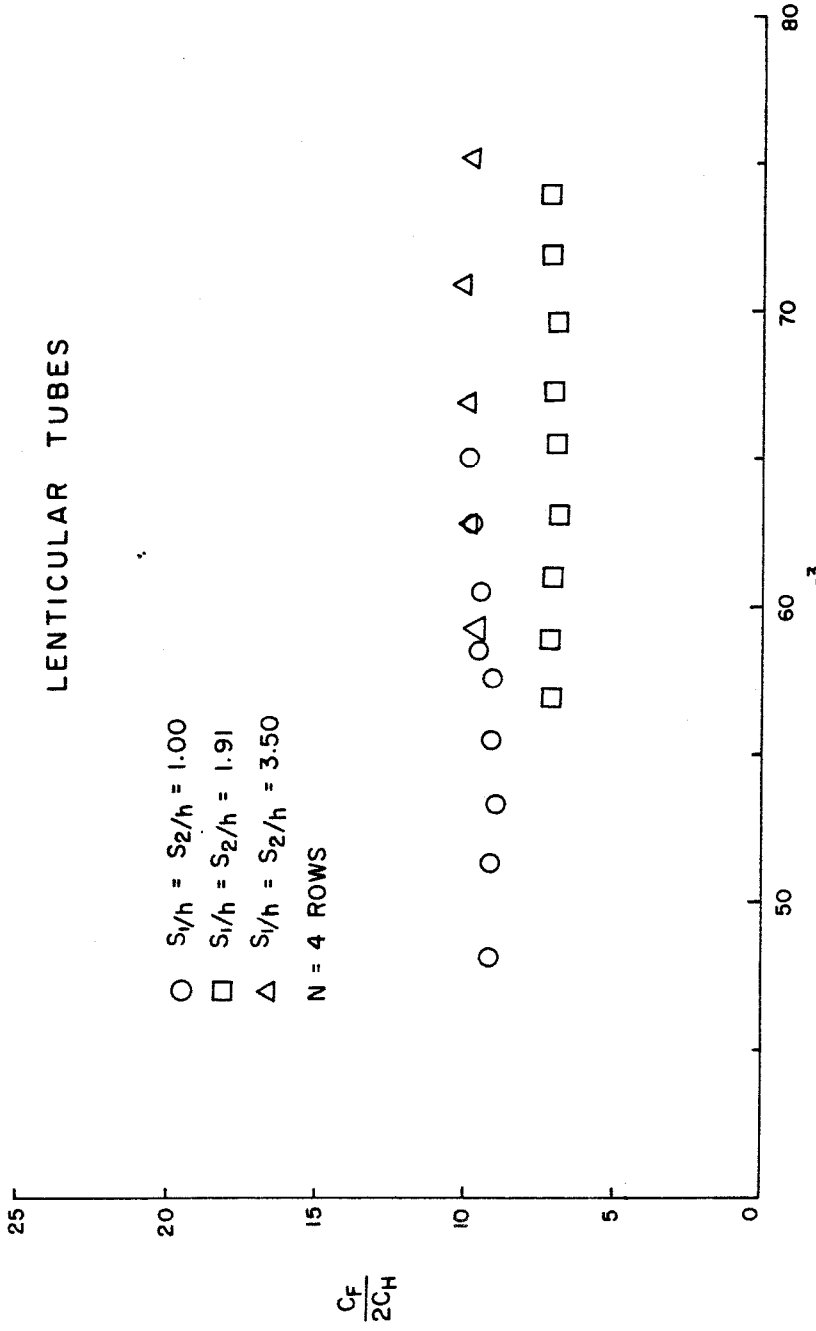

Figure 19. $C_f/2C_h$ vs. R_e N = 4 Lenticular Tubes

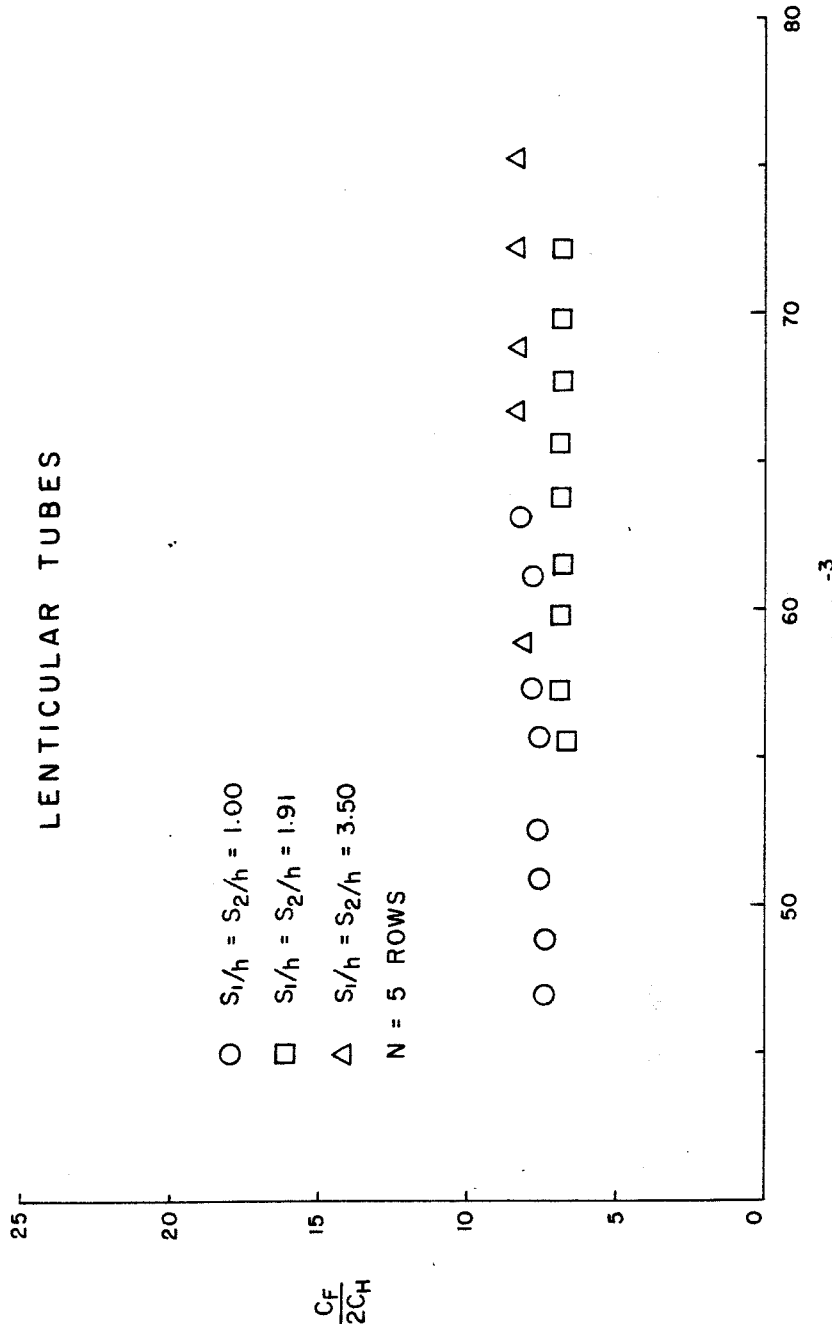

Figure 20. $C_f/2C_h$ vs. R_e N = 5 Lenticular Tubes

the change is that a more universal definition of Reynolds number has an advantage when comparing heat exchangers of different geometries. Primes are used to denote the new definitions.

The effect of increasing the number of rows can be seen in the following figures.

Figures 21, 22, and 23 are for the configurations with $s_1 = s_2 = 1$ h. There is a slight decrease in pressure loss with increasing number of rows as shown in figure 21. The plot of C_h' vs. R_e' in figure 22 shows some improvement with the addition of more rows. The ratio of $C_f'/2C_h'$ (figure 23) shows an improvement in performance with the addition of more rows. The greatest improvement is between 3 and 4 rows with less improvement between 4 and 5 rows. The data for circular tubes show that $C_f'/2$ is independent of the number of rows and that C_h' depends on N only for cases with less than 10 rows with C_h' increasing with each additional row until a constant value is reached[3]. These trends do not appear in these experiments.

Figures 24, 25, and 26 are for $s_1 = s_2 = 1.91$ h. With 3 and 4 rows there were no separation bubbles. However, addition of the fifth row produced a downstream separation region and only a small improvement over 4 rows. This can be seen in figure 24 ($C_f'/2$ vs R_e') and figure 26 ($C_h'/2C_h'$ is R_e'). The Stanton number was nearly the same for all these cases.

Similar curves for $s_1 = s_2 = 3.50$ h are figures 27, 28, and 29. There was no separation bubble present for any of these cases and the effect of adding more rows is clearly seen in figure

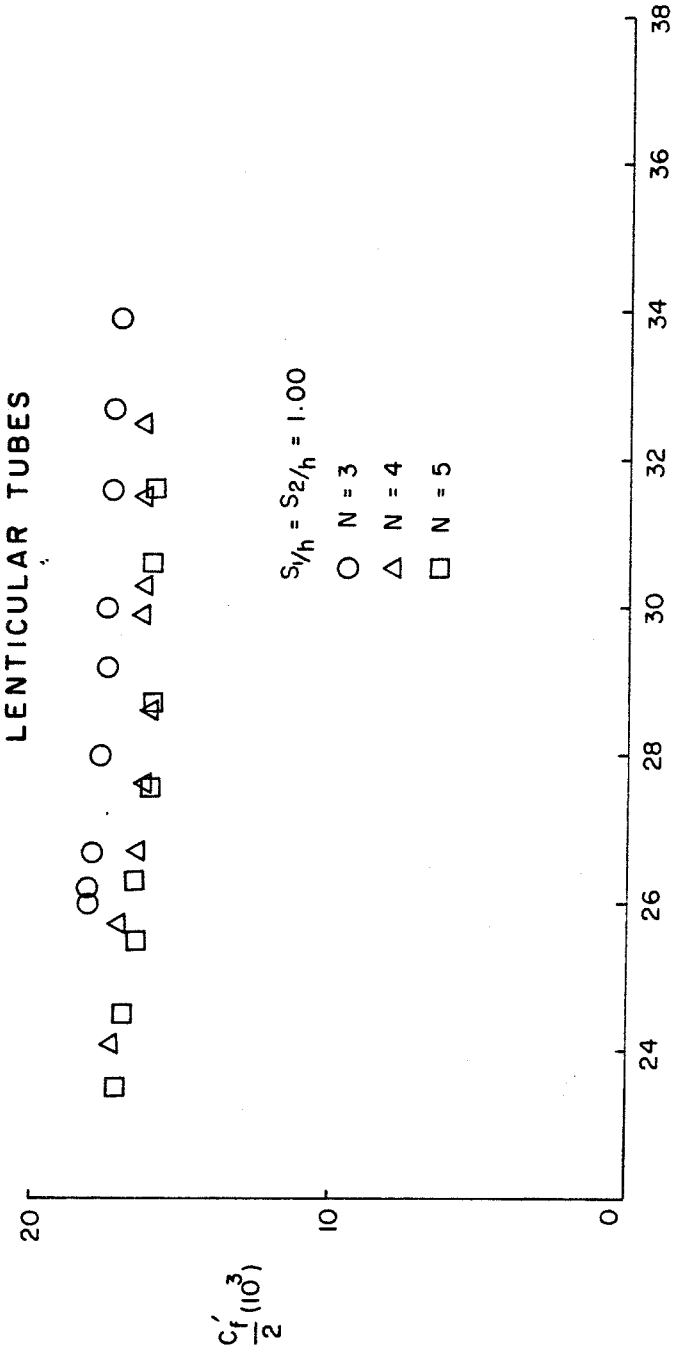

Figure 21. C_f' vs. R_e' $s_1 = s_2 = 1.00$ h

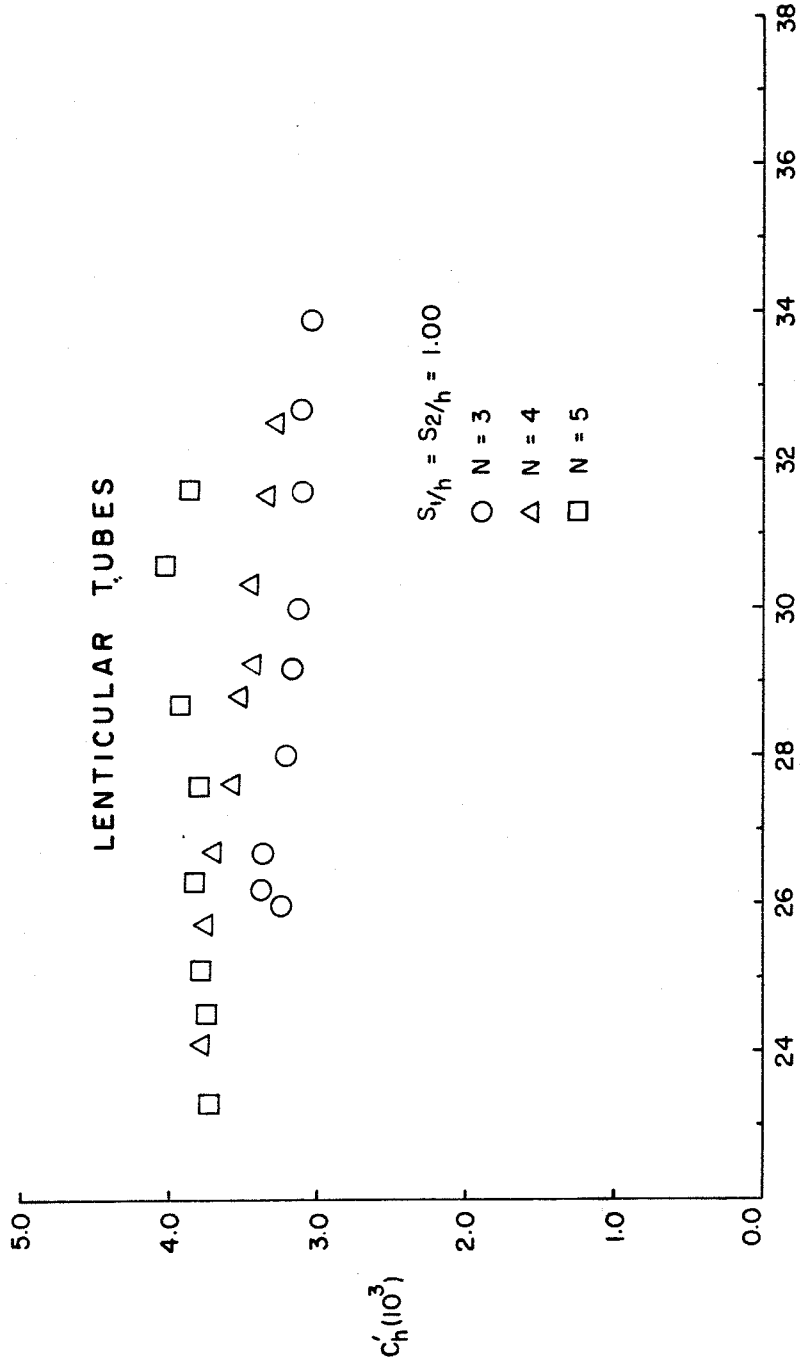

Figure 22. C'_h vs. R'_e $s_1 = s_2 = 1.00$ h

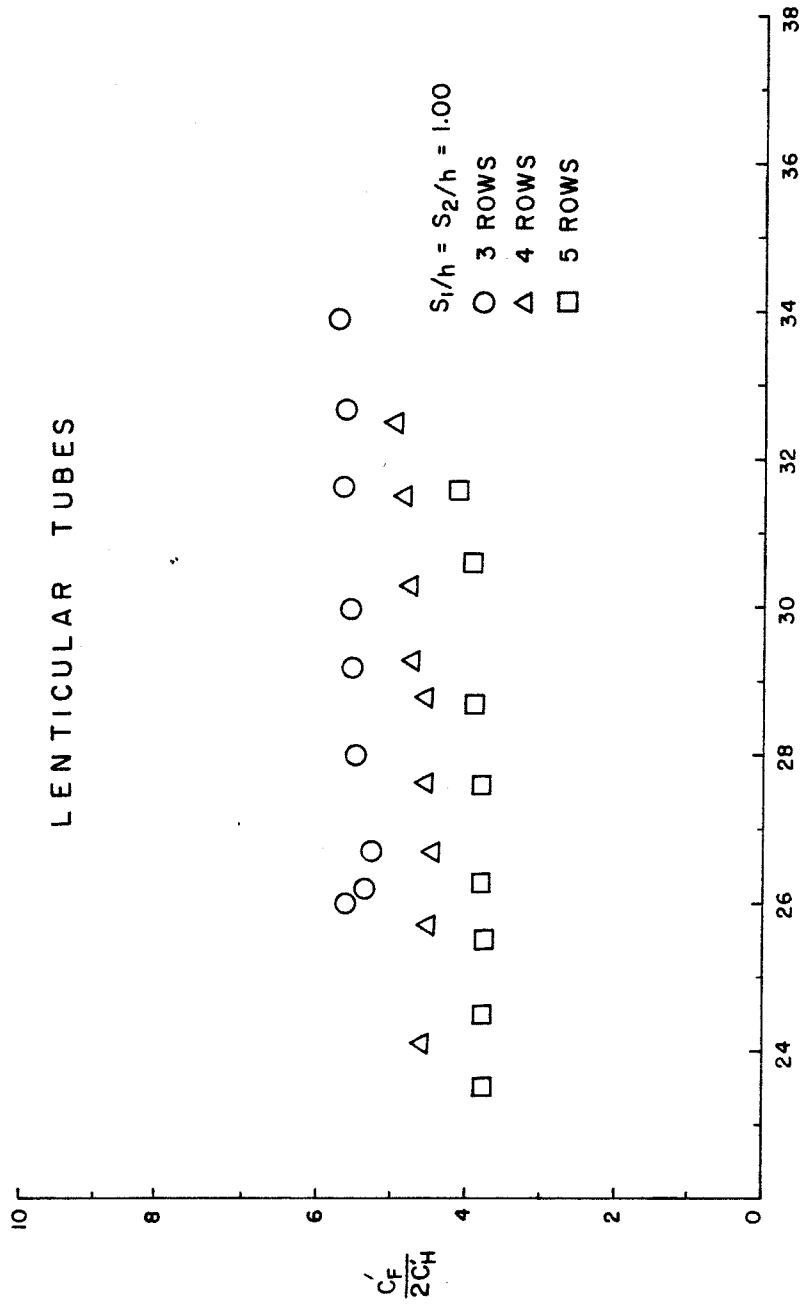

Figure 23. $C_f'/2C'_h$ vs. R'_e $s_1 = s_2 = 1.00$ h

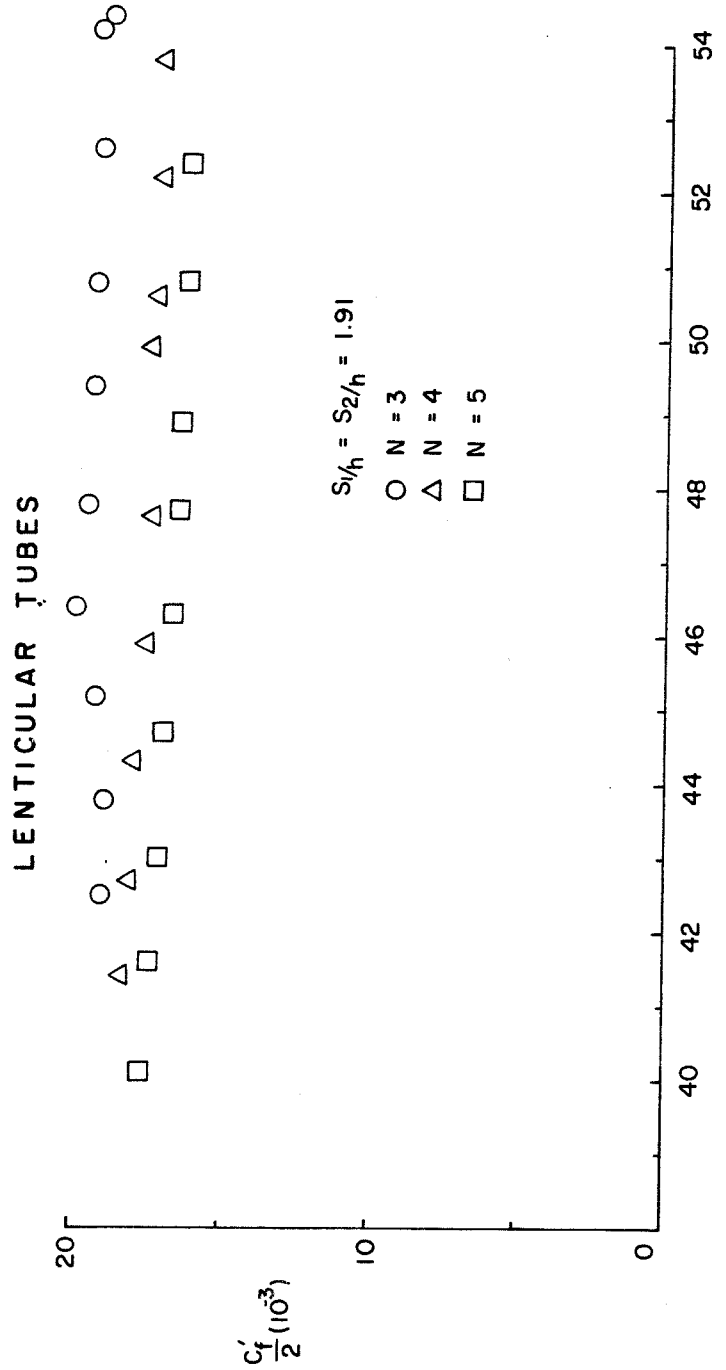

Figure 24. $C_f'/2$ vs. R_e' $s_1 = s_2 = 1.91$ h

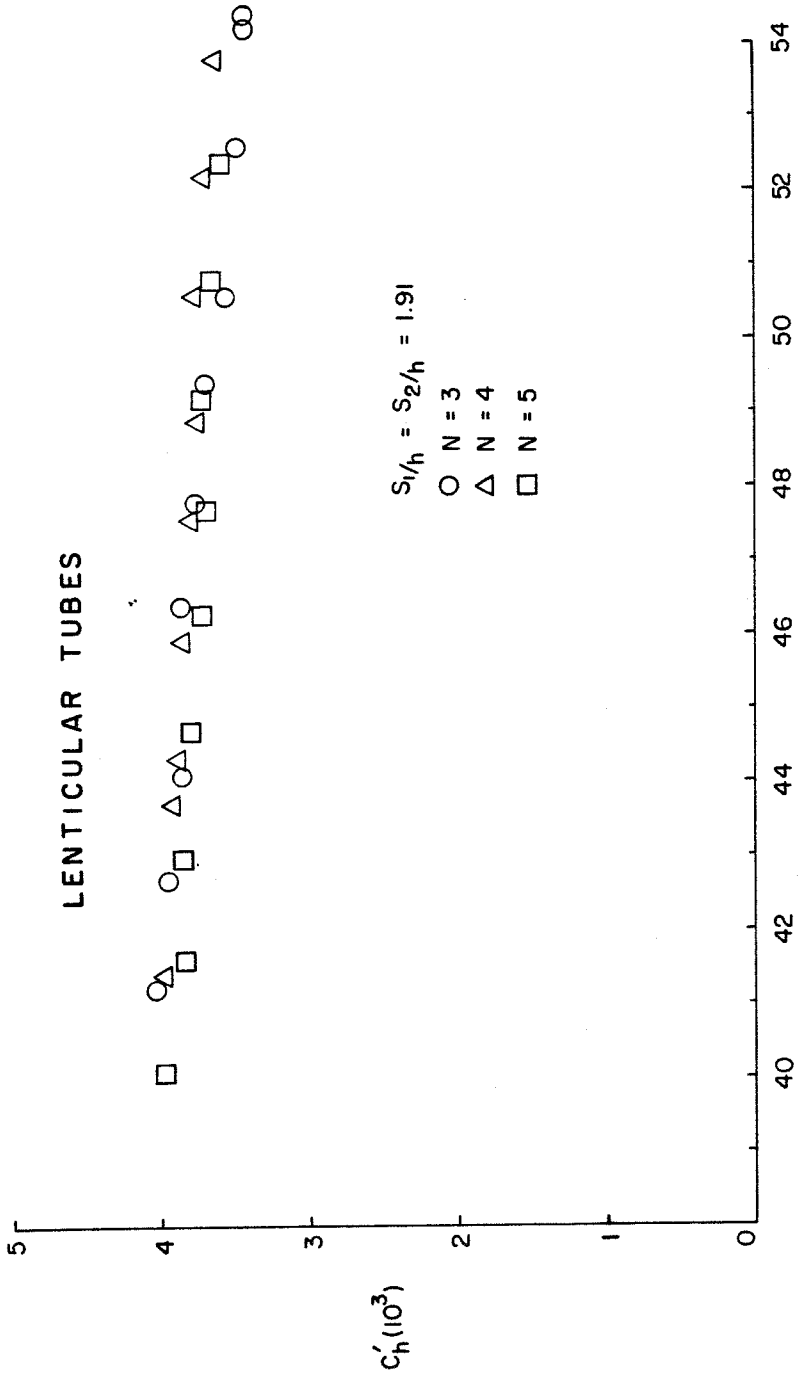

Figure 25. C'_h vs. R'_e $s_1 = s_2 = 1.91$ h

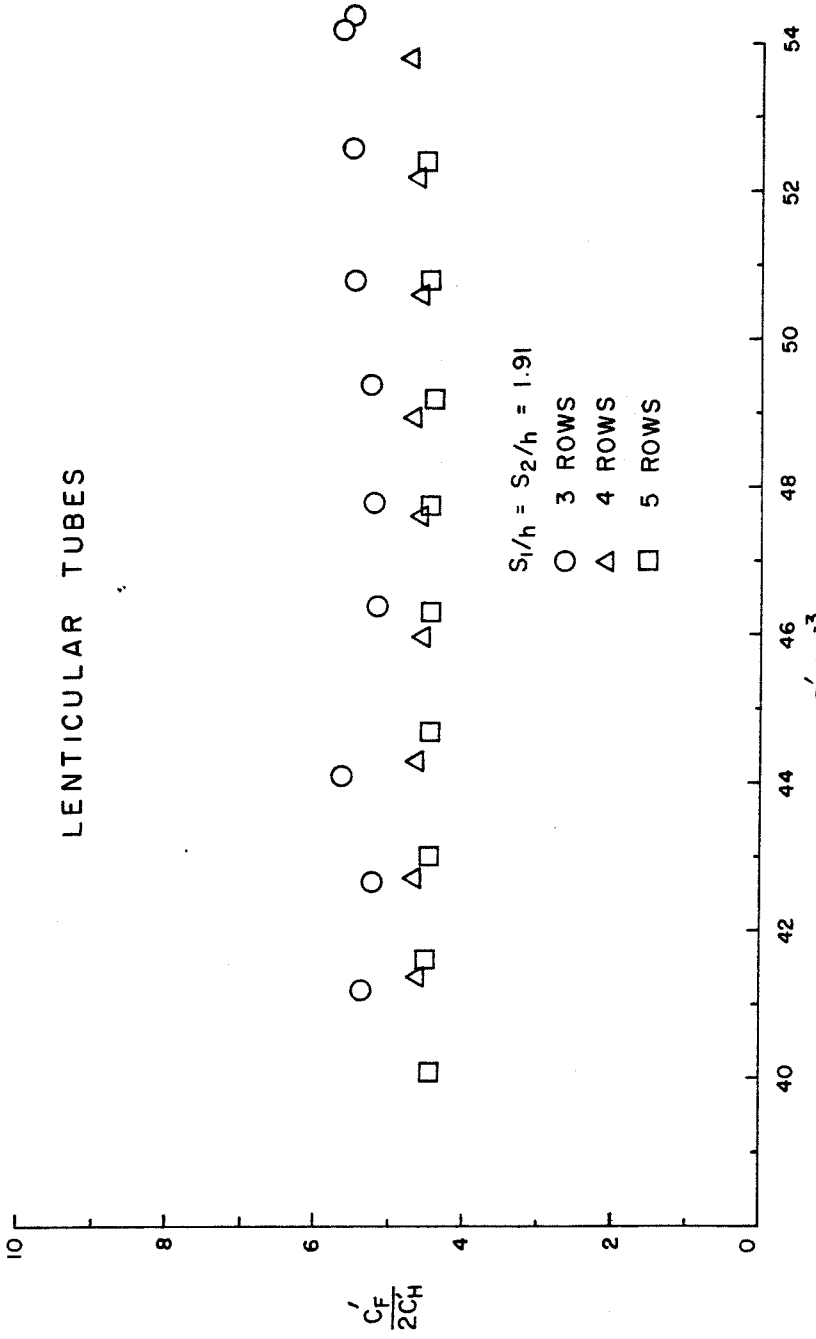

Figure 26. $C_f'/2C_h'$ vs. R_e' $s_1 = s_2 = 1.91$ h

27 where there is an appreciable decrease in drag with the addition of more rows. The heat transfer shows a very slight increase in figure 28 for 4 and 5 rows over 3 rows, but little difference between 4 and 5. And in figure 29 the figure of merit improves with increasing number of rows.

A highly speculative explanation for the dramatic decrease in drag with the addition of more rows for this spacing is that laminar separation occurs on the first rows resulting in greater losses due to the larger wakes. As the number of rows is increased the tubulence from the preceding rows prevents the laminar separation of subsequent rows resulting in lower pressure losses for the latter rows. Thus with the addition of more rows the surface area would increase faster than the pressure losses and the value of $C_f/2$ would decrease.

Another phenomenon observed with some configurations of the lenticular tubes was the existence of a noticeable tone different from the noise normally associated with the operation of the tunnel. This tone did not exist for all spacings and velocities but was particularly noticeable for $s_1 = s_2 = 3.5$ h with 3 rows and high Reynolds number. As the Reynolds number was decreased the tone became less noticeable and may have changed pitch. For $R_e = 76.5\ (10^3)$ a spectrum analyzer measured a frequency of 1420 Hz. If this tone was due to a resonance caused by the shedding of vortices along the length of the tube that were out of phase with each other then the expected frequency based on the 9 in. height of the tubes would be 1510 Hz which is 6%

greater than the measured value.

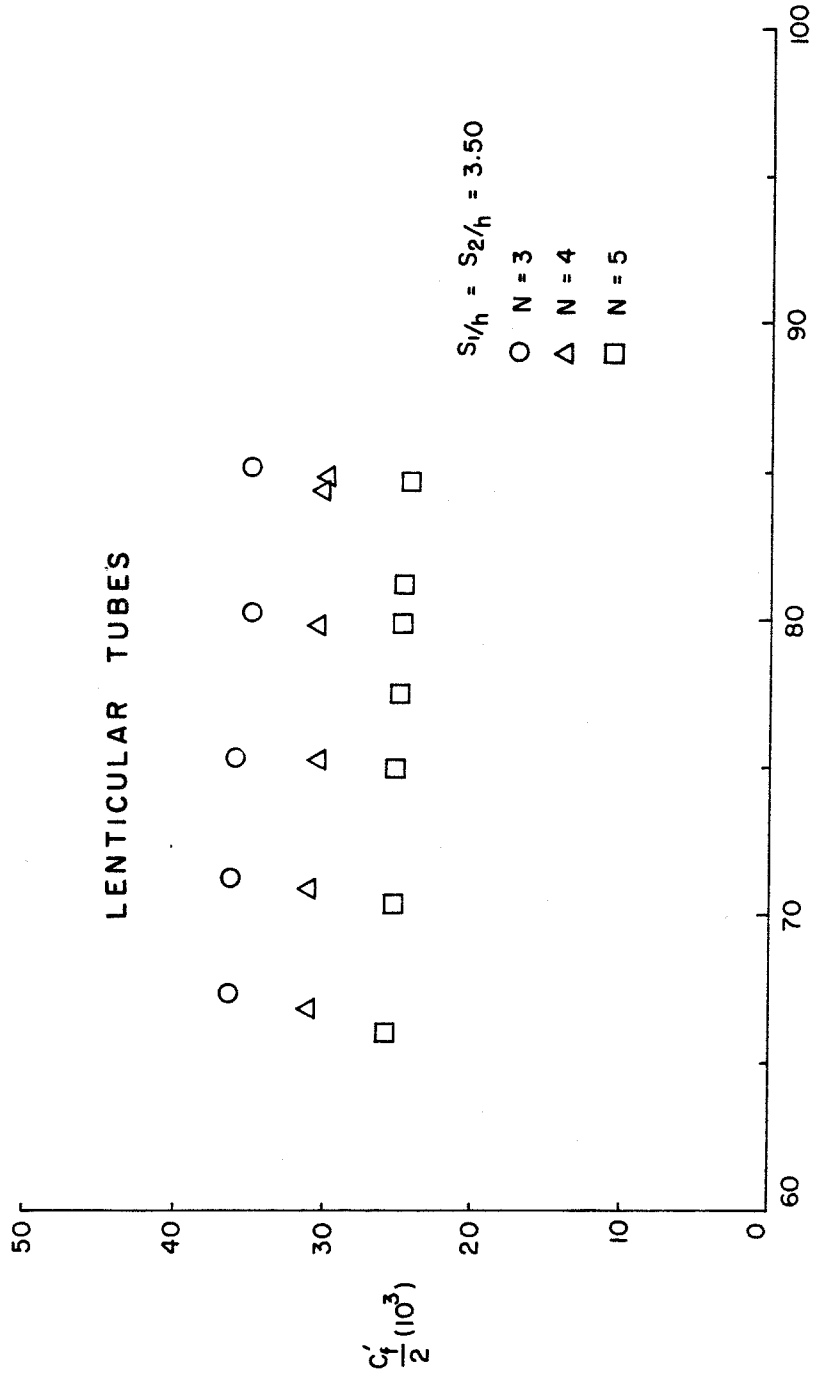

Figure 27. $C'_f/2$ vs. R'_e $s_1 = s_2 = 3.50$ h

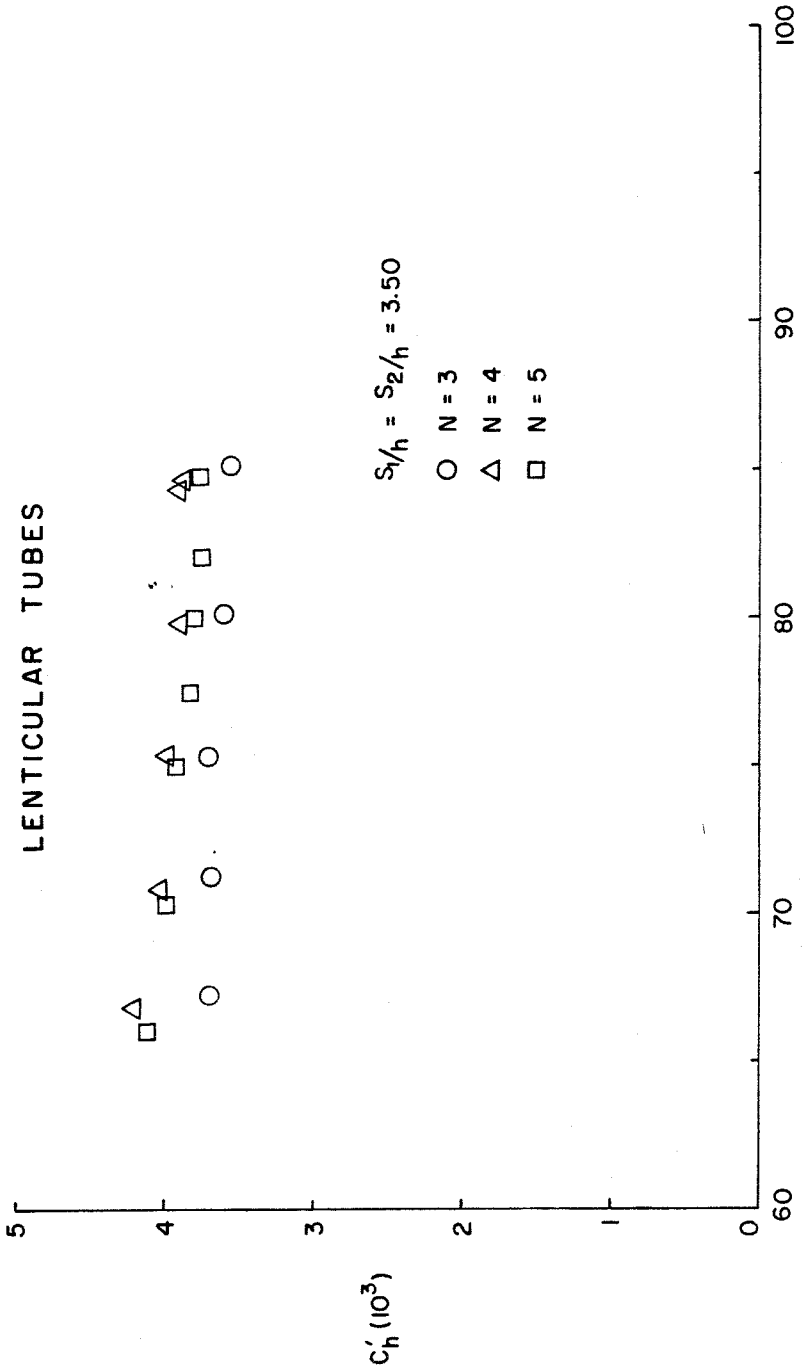

Figure 28. C'_h vs. R'_e $s_1 = s_2 = 3.50$ h

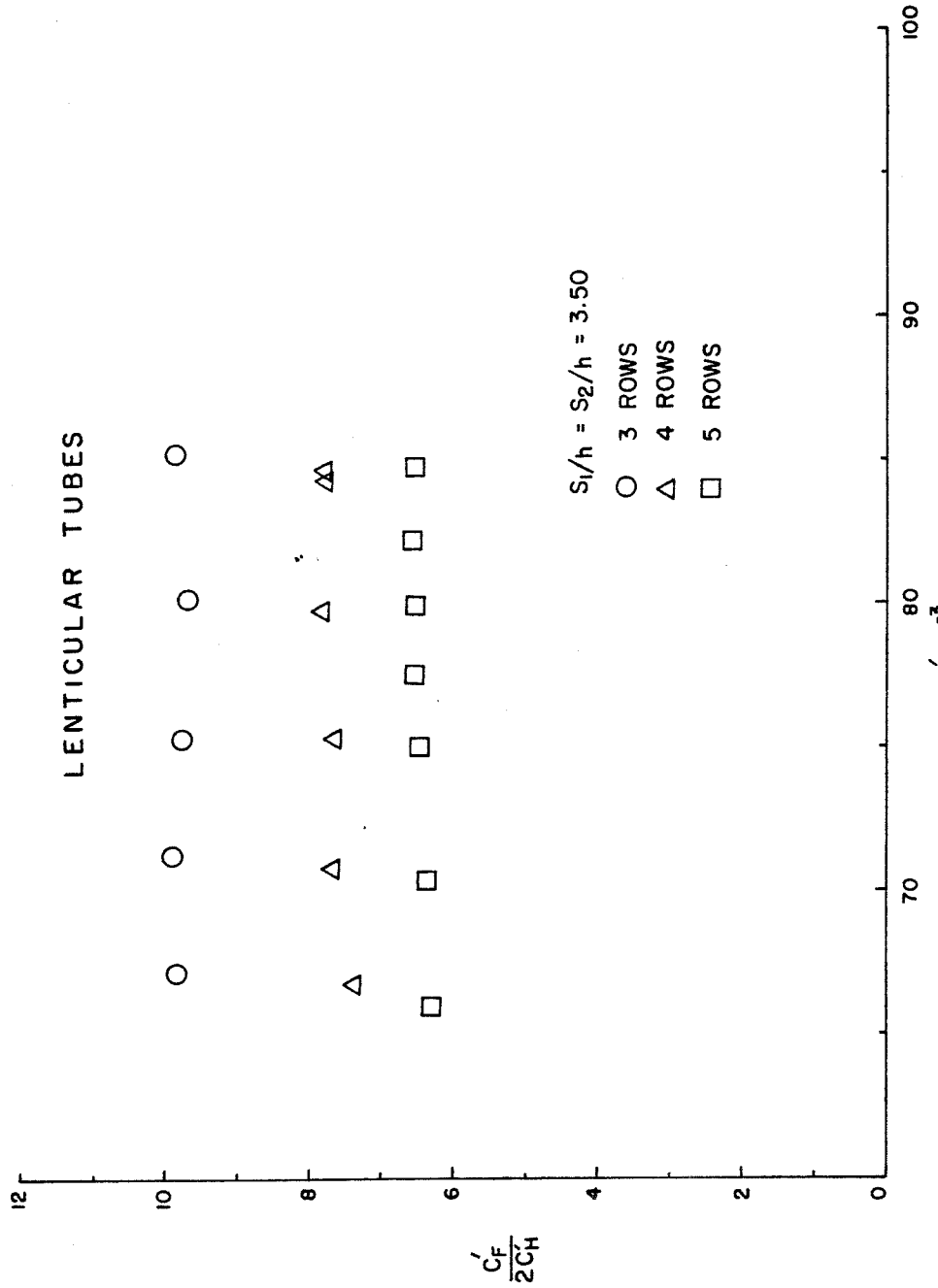

Figure 29. $C'_f/2C'_h$ vs. R'_e $s_1 = s_2 = 3.50$ h

VII. EFFECT OF VARIATION OF REYNOLDS NUMBER ON LENTICULAR TUBE HEAT EXCHANGER

In the experiment described above the Reynolds number could be varied only over a small range by opening or closing bypass ports. To determine the effect of much larger variations an orifice plate was installed at the diffuser exit to reduce the flow through the fan. By changing the size of the hole in the orifice plate in combination with the normal velocity control system, experiments could be performed over a wider range of Reynolds number. These experiments were run with $s_1/h = s_2/h = 1.91$ only. This configuration was the one that gave the best performance in the previous test.

Figure 30 is a plot of $C_f'/2$ vs. R_e'. A best fit of a simple power relationship is crawn through the points. The plot of C_h' vs. R_e' is shown in figure 31 again with a simple power curve fit. Both $C_f'/2$ and C_h' are increasing rapidly with decreasing Reynolds number. Figure 32 shows C_h' is increasing at a greater rate so that performance improves with the lower Reynolds numbers. The same trend holds for other arrangements as will be seen in the next section.

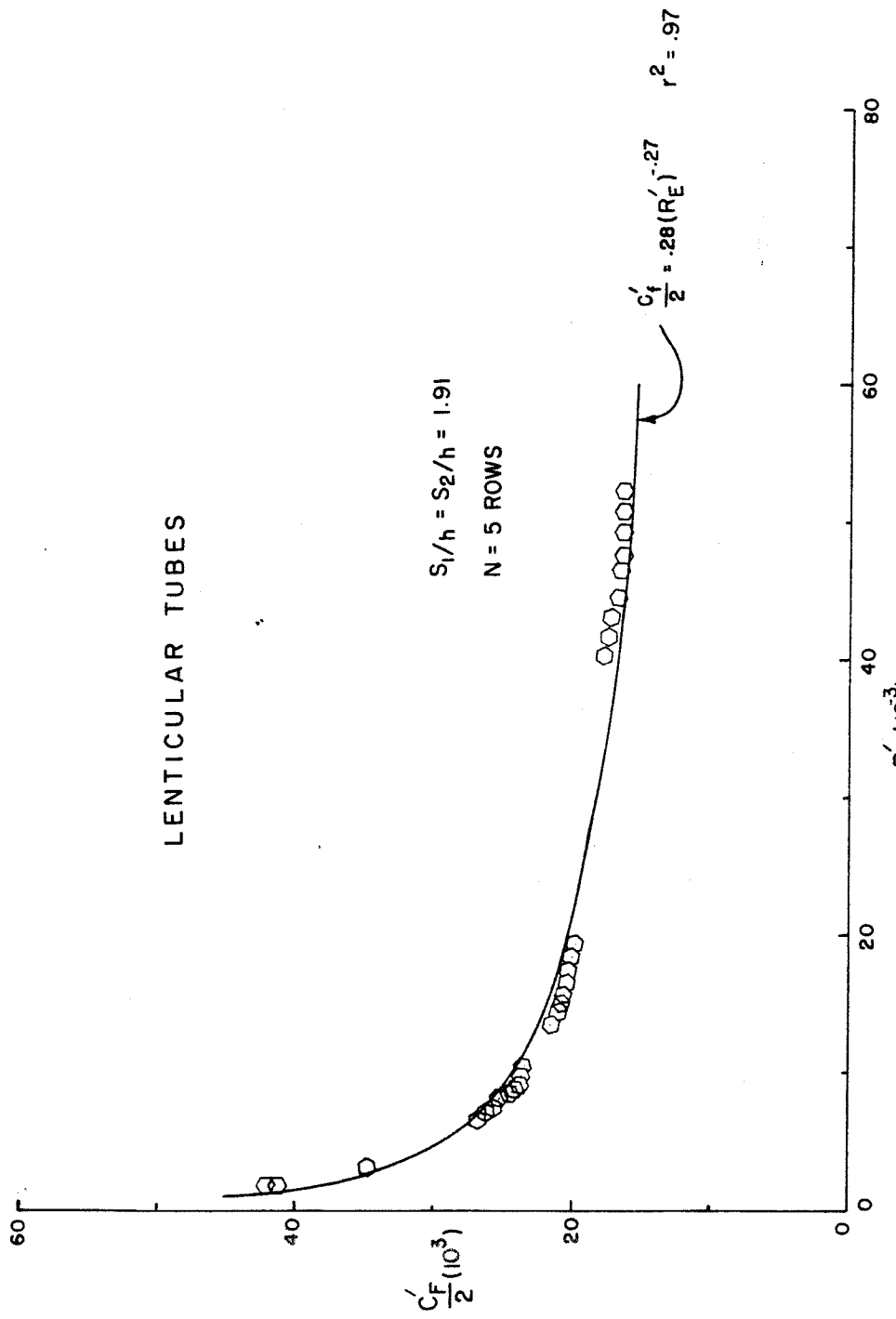

Figure 30. $C'_f/2$ vs. R'_e Extended Reynolds Number
$s_1 = s_2 = 1.91$ h N = 5

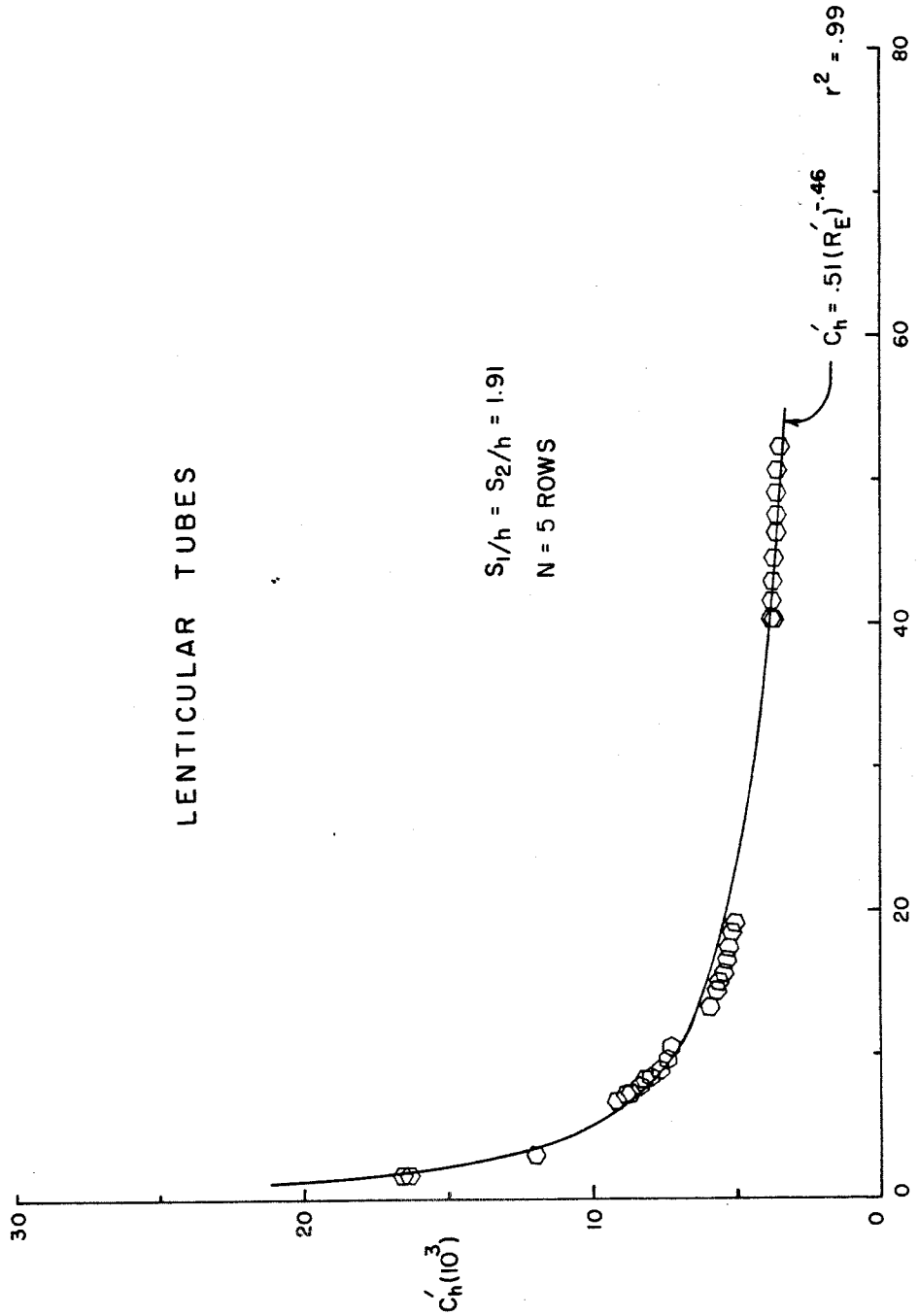

Figure 31. C_h' vs. R_e' Extended Reynolds Number
$s_1 = s_2 = 1.91$ h N = 5

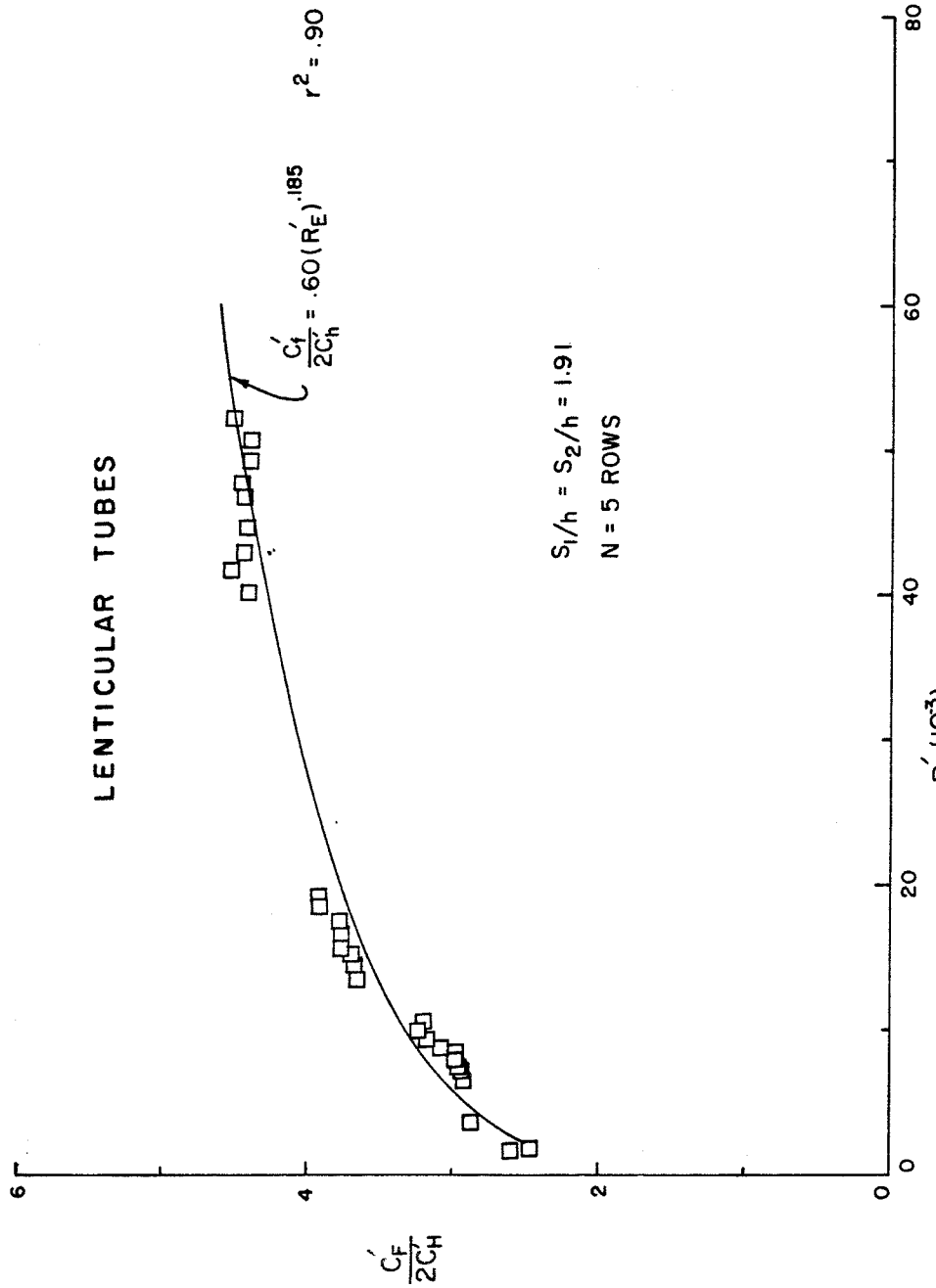

Figure 32. $C_f'/2C_h'$ vs. R_e' Extended Reynolds Number
$s_1 = s_2 = 1.91$ h N = 5

VIII. COMPARISON OF HEAT EXCHANGER CONFIGURATIONS

The characteristics desired in a heat exchanger depend very much on what mission it is to be designed for. In this investigation the ratio $C_f/2C_h$ has been used as a figure of merit to compare heat exchangers of the same type. However, this ratio is dependent on the geometry and Reynolds number which in turn depend on the application. Hence it is not possible in general to find a criterion for comparing different types of heat exchangers and pronounce one superior to the other. Here no attempt will be made to select one type of heat exchanger over another but information on the arrangements investigated will be compared with the available data for more conventional types of similar size.

By far the largest number of experiments on heat exchangers have been for the in-line and staggered arrangements of circular cylinders of figures 2 and 3. Extensive research on heat transfer and pressure loss for both in-line and staggered layouts with different pitch-to-diameter ratios was undertaken for the Babcock and Wilcox Company by Pierson, Huge, and Grimison in 1936[4, 5, 6]. Correlations of these data with the work of others have been done for heat transfer by Fishenden and Saunders[7] and for pressure loss by Jakob[8]. More recently Zhukauskas[9] has performed many heat transfer experiments with single tubes and banks of cylinders. The effect of the number of rows has been investigated by Kays[10, 11], and also presented in Kreith[3].

The data show that staggered layouts have high Stanton numbers but also very high pressure loss coefficients so that the ratio of $C_f/2C_h$ turns out to be lower for in-line layouts although the latter have lower values of C_h. Because of this the in-line arrangement was used as a standard for comparison with the lenticular shaped tubes.

The last figure (33) is a comparison of these data with the results for lenticular tube heat exchanger. The hexagons represent the experiment described above for $s_1 = s_2 = 1.91$ h and 5 rows. This was the case with the lowest values of $C_f/2C_h$. The ratio of frontal area to minimum free area, A/A_{min}, was 1.52 and the value of S/A was 14.3. The ratio of the square of the surface area per unit height to volume per unit height, $(S/H)^2/(V/H)$, was 73.9.

For comparison an in-line bank of circular tubes with a transverse spacing of $s_t/d = 3$, a longitudinal spacing $s_l/d = 1.25$, and corrected for 5 rows was picked since it had the lowest values of C_f/C_h appearing in Pierson's data. For this configuration $S/A = 5.24$, $A/A_{min} = 1.50$, and $(S/H)^2/(V/H) = 13.7$.

At the higher Reynolds numbers the lenticular tubes are slightly better but the two are very close together. The lenticular tubes have higher surface area/frontal area and are much more compact.

Besides the in-line tube data of Pierson and Zhukauskas figure 33 also has data from Kays and London[12] for a staggered arrangement of oval tubes made of flattened circular cylinders.

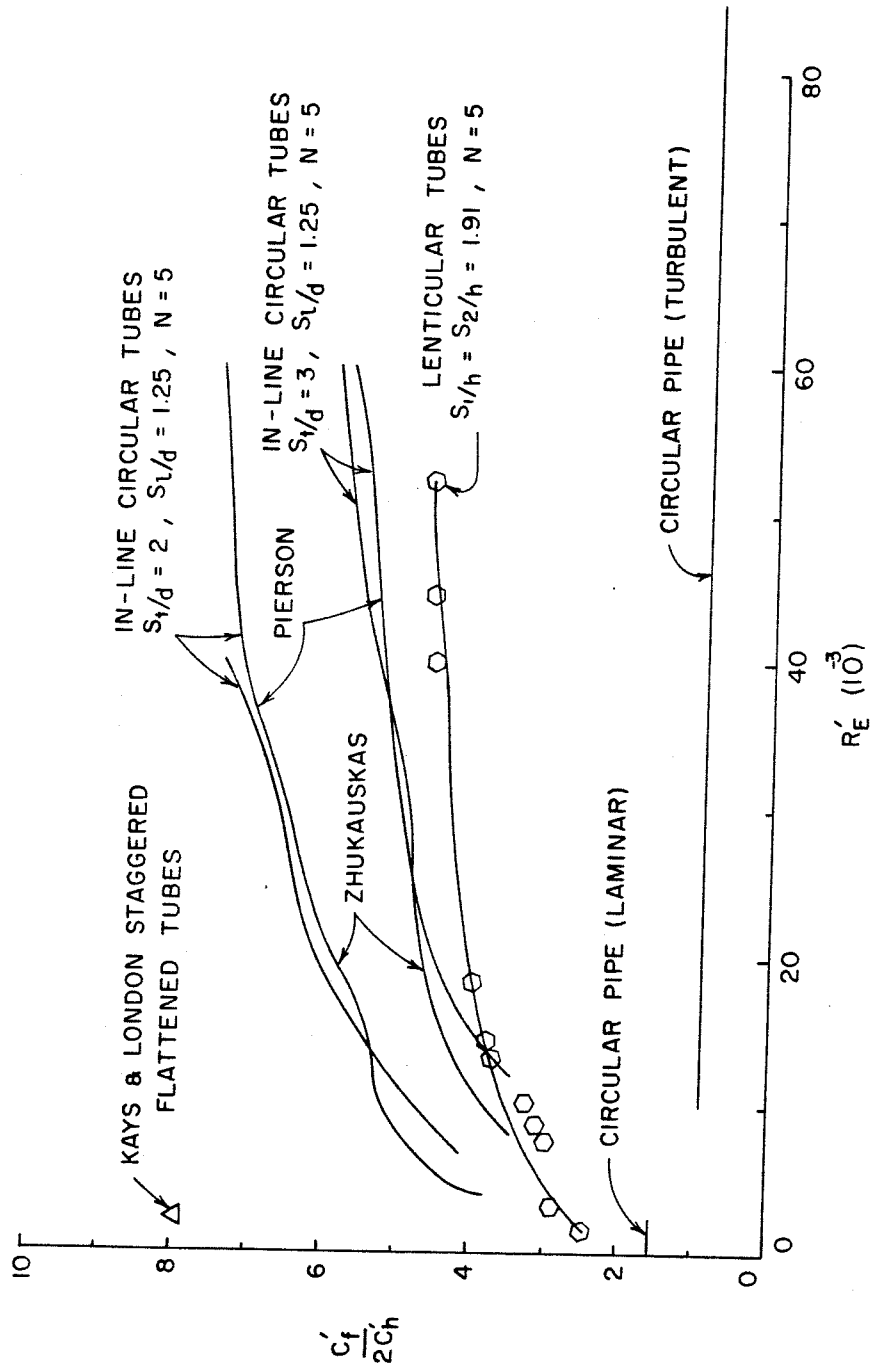

Figure 33. Comparison of Different Types of Heat Exchangers

This arrangement is similar to the lenticular tube heat exchanger but has larger variations of nominal level velocity in the tube bank. Information is available only for one spacing with A/A_{min} = 2.59 and a surface area per unit volume of 108 ft^2/ft^3. The tubes were .315 in. long, .127 in. thick and had a transverse spacing of .222 in. and a longitudinal spacing of .344 in. It is inferior in performance to the other arrangements.

For reference, the curve for turbulent flow of air in a circular pipe is shown. This plot is simply the result of Reynolds' analogy using the mean velocity as a reference or $C_f/2C_h = P_r$ with $P_r = .7$ for air.

From figure 16 the sawtooth pattern heat exchanger for $\phi = 15^o$ has an average value of $C_f/2C_h$ equal to 17.5 for a Reynolds number based on the gap spacing of about 30 (10^3). This is much higher than corresponding values for lenticular tubes as shown in figures 18, 19 and 20. Performance improved with decreasing angle, however how practical this may be in an application is uncertain Since the total heat transferred from a single row is low many rows would be needed in an actual design. There would not appear to be any advantage to having many closely spaced sawtooth rows over the more conventional in-line and staggered arrangements.

IX. CONCLUSION

The purpose of these experiments was to investigate the performance of two unconventional crossflow heat exchanger configurations to determine if these might lead to a decrease in the pressure loss of the flow through the heat exchanger for a given heat transfer rate. As stated earlier it is difficult to compare different types of heat exchangers without considering the design requirements of their intended applications. In this work the ratio of friction coefficient to heat transfer coefficient in the form $C_f/2C_h$ was chosen as a figure of merit to be used in comparing different geometries of both forced and natural draft heat exchangers.

The first set of experiments with circular tubes arranged in a sawtooth pattern revealed that the ratio of $C_f/2C_h$ was lower for the configuration with the smaller angle ϕ. However the measured values of $C_f/2C_h$ were still higher than those obtainable with more conventional heat exchangers and the only possible advantage of the sawtooth pattern might be that it has a high heat transfer surface for a given volume. Further investigation of the sawtooth heat exchanger did not seem warranted.

The second set of experiments with the lenticular shaped tubes spaced so that the flow area between them was nearly constant through the tube bank gave appreciably lower values of $C_f/2C_h$ than more conventional heat exchangers with tubes of circular cross section, especially at higher Reynolds numbers. The better performance of the lenticular tubes compared with

circular tubes must be balanced against the disadvantage of a shape that is more difficult to manufacture and fit and is not as good for a very large pressure difference of the two streams.

The results of these experiments show a need for further investigation at lower Reynolds numbers (in the laminar and transitional regimes of the cross flow). The scale and/or instrumentation sensitivity of the existing equipment must be modified for such experiments. The effect of adding fins to the outside of the lenticular tubes would also be of considerable interest.

LIST OF SYMBOLS

A	frontal area of heat exchanger
$C_f/2$	drag coefficient
C_h	Stanton number
c	chord
c_p	specific heat at constant pressure
d	circular tube diameter
g	acceleration due to gravity
h	heat transfer coefficient, half thickness of lenticular tubes
H	height of natural draft heat transfer tower, height of heat exchanger
k	thermal conductivity
ℓ	length of heat exchanger
$\dot{m}$	mass flow rate
N	number of rows
P	pressure
P_r	Prandtl number
$\dot{Q}$	heat flow rate
$\dot{q}$	heat flow rate per unit surface area
R	gas constant
R_e	Reynolds number
S	surface area
s_ℓ	longitudinal tube spacing of conventional circular tube heat exchanger
s_t	transverse tube spacing of conventional circular tube heat heat exchanger

s_1 distance from side of lenticular tube to centerline of adjacent tube in next row

s_2 minimum distance between lenticular tube and adjacent tube in next row

s space between sawtooth pattern tubes

T temperature

t wall thickness

u velocity

V volume of heat exchanger

$\dot{W}$ pumping power

W width of heat exchanger

x horizontal distance

y vertical distance

α $C_h S/A$

γ ratio of specific heats

ϵ heat exchanger effectiveness

ξ x/ℓ

κ thermal diffusivity

ϕ half angle of sawtooth pattern tubes

u coefficient of viscosity

μ kinematic viscosity

ρ density

REFERENCES

1. Fraas, A. and Ozisik, M., Heat Exchanger Design, John Wiley and Sons, 1965, pp. 1-2.
2. Reynolds, O., "The Extent and Action of the Heating Surface of Steam Boilers," Proceedings of the Literary and Philosophical Society of Manchester," vol. 14, 1874, pp. 7-12.
3. Kreith, F., Principles of Heat Transfer, Intext Educational Publisher, 1973, pp. 473-483.
4. Pierson, O., "Experimental Investigation of Influence of Tube Arrangement on Convection Heat Transfer and Flow Resistance in Cross Flow of Gases Over Tube Banks," Trans. A.S.M.E., vol. 59, 1937, pp. 563-572.
5. Huge, E., "Experimental Investigation of Effects of Equipment Size on Convection Heat Transfer and Flow Resistance in Cross Flow of Gases over Tube Banks," Trans. A.S.M.E., vol. 59, 1937, pp. 573-582.
6. Grimison, E., "Correlation and Utilization of New Data on Flow Resistance and Heat Transfer for Cross Flow of Gases over Tube Banks," Trans. A.S.M.E., vol. 59, 1937, pp. 583-594.
7. Fishenden, M. and Saunders, O., An Introduction to Heat Transfer, Oxford: Clarendan Press, 1950, pp. 132-145.
8. Jakob, M., "Heat Transfer and Flow Resistance in Cross flow of Gases over Tube Banks," Trans. A.S.M.E., vol. 60, 1938, pp. 384-380.

REFERENCES (CONT'D)

9. Zhukauskas, A., "Heat Transfer in Banks of Tubes," Mintis, Vilnius, Lithuania, 1968.

10. Kays, W. and Lo, R., "Basic Heat Transfer and Flow Friction Design Data for Gas Flow Normal to Banks of Staggered Tubes - Use of a Transient Technique," Tech. Rep. 15, Navy Contract N6-onr -251T.O.6., Stanford University, 1952.

11. Kays, W., "Basic Heat Transfer and Flow Friction Design Data for Gas Flow Normal to Banks of In-line Circular Tubes - Use of a Transient Technique," Tech. Rep. 15, Navy Contract N6-onr -251 T.O. 6, Stanford University, 1954.

12. Kays, W. and London, A., Compact Heat Exchangers, McGraw-Hill Book Company, 1964, p. 165.

APPENDIX A

The use of blocks of aluminum honeycomb as a thermal mass to reduce temperature fluctuations in the entering flow is described in the text. The performance of the thermal mass can be estimated by modeling the flow through the honeycomb with flow through the interior of a bundle of pipes.

The heat equation for flow inside a pipe of radius a, length ℓ, and thickness t_w is

$$\frac{\partial T}{\partial t} + u \frac{\partial T}{\partial x} = \kappa \frac{1}{r} \frac{\partial}{\partial r} \left(r \frac{\partial T}{\partial r}\right) \quad 0 \leq r \leq a$$

with the boundary condition that the heat conducted into the wall is

$$\rho_w \, c_w \, t_w \, \tfrac{1}{2} \frac{\partial T_w}{\partial t} = -k \left(\frac{\partial T}{\partial r}\right)_{r=a}$$

where ρ_w is the density of the wall material, c_w is the specific heat, and T_w is the wall temperature.

The velocity profile inside the pipe will be that for Poiseville flow

$$u = 2 \bar{u} \left[1 - \left(\frac{r}{a}\right)^2\right]$$

$\bar{u}$ is the mean velocity.

Assume the inlet temperature is a periodic function of time with frequency ω

$$T = T_o + \Delta T \, e^{i\omega t} \quad \text{at } x = 0 \, .$$

Let $\eta \equiv \frac{r}{a}$ and $\xi \equiv \frac{x}{a}$ and assume the temperature distribution through the pipe is

$$T = T_o + \Delta T \, R(\eta) \, X \, (\xi) \, e^{i\omega t}$$

Substituting into the heat equation

$$\Delta T R X i\omega e^{i\omega t} + 2\bar{u}(1-\eta^2)\Delta T R X' \frac{1}{a} e^{i\omega t} = \kappa \frac{1}{a^2} \quad R'' + \frac{1}{\eta} R' \quad X e^{i\omega t} \Delta T$$

or

$$i\omega RX + \frac{2\bar{u}}{a} (1-\eta^2) X'R = \frac{\kappa}{a^2} \frac{1}{\eta} (\eta R') \quad X$$

Separation of variables given

$$\frac{1}{\eta (1-\eta^2) R} (\eta R')' - i\omega \frac{a^2}{\kappa} \frac{1}{1-\eta^2} = 2 \frac{\bar{u}a}{\kappa} \frac{X'}{X} = -\Lambda$$

Let

$$\beta \equiv \frac{\omega a^2}{\kappa} \qquad \alpha \equiv 2 \frac{\bar{u}a}{\kappa}$$

Then

$$\frac{1}{\eta} \frac{d}{d\eta} (\eta \frac{dR}{d\eta}) + \quad \Lambda \quad (1-\eta^2) - i\beta \quad R = 0$$

and

$$X' + \frac{\Lambda}{\alpha} X = 0$$

The boundary condition becomes

$$i\omega \rho_w c_w t_w \tfrac{1}{2} \Delta T R(1) X(\xi) e^{i\omega t} = -kR'(1) X(\xi) \Delta T \frac{1}{a} e^{i\omega t}$$

since

$$T_w = T_o + \Delta T \; R(1) X(\xi) \; e^{i\omega t}$$

Thus

$$R(1) = \frac{2i\kappa \rho c_p}{a\omega \rho_w c_w t_w} \quad R'(1)$$

Let

$$K \equiv \frac{\omega a^2}{2} \frac{\rho_w c_w t_w}{\rho c_p a}$$

then

$$R(1) = \frac{i}{K} R'(1)$$

Also from symmetry

$$R'(0) = 0$$

The solutions are

$R = R^{(1)}, R^{(2)}, - - -$ for $\Lambda = \Lambda^{(1)}, \Lambda^{(2)}, - - -$

and

$X^{(n)} = e^{-\frac{\Lambda^{(n)}}{\alpha} \xi}$ etc.

If the least value of the real part of Λ is known the change in amplitude of the temperature fluctuation along the length of the thermal mass would be given by the above equation. An iterative analytical solution for Λ is possible using Rayleigh's method.

Recall that the equation for $R(\eta)$ and boundary conditions are

$$\frac{d}{d\eta}\left(\eta \frac{dR}{d\eta}\right) = -\left[\Lambda \eta (1-\eta^2) - i\beta\eta\right] R$$

$$R'(0) = 0$$

$$R(1) = \frac{i}{K} R'(1)$$

As a first approximation the simplest polynomial satisfying the boundary conditions was chosen, i.e.

$$R_o = \eta^2 + B$$

where $$B = \frac{2i - K}{K}$$

Then find second approximation by

$$\frac{d}{d\eta}\left(\eta \frac{dR_1}{d\eta}\right) = - \left[\Lambda \eta (1-\eta^2) - i\beta\eta\right] R_o$$

So

$$R_1 = - \frac{\Lambda}{4}\left[B\eta^2 - \frac{B-1}{4}\eta^4 - \frac{\eta^6}{9}\right] + \frac{i\beta}{4}\left[B\eta^2 + \frac{\eta^4}{4}\right] + C$$

$$C = \Lambda\left[-\frac{11}{72} + \frac{13}{24}\frac{i}{K} + \frac{1}{2K^2}\right] + i\beta\left[\frac{3}{16} - \frac{1}{K^2} - \frac{3}{4}\frac{i}{K}\right]$$

To find Λ let

$$\int_o^1 R_o (1-\eta^2)\,\eta\, d\eta = \int_o^1 R_1 (1-\eta^2)\,\eta\, d\eta$$

then

$$\Lambda = \frac{-\frac{7}{24}\frac{\beta}{K} - \frac{1}{3} + i\frac{\beta}{2K^2} - \frac{11}{192}\beta + \frac{1}{K}}{\frac{1}{4K^2} - \frac{7}{160} + i\frac{19}{46K}}$$

The following values were selected for the thermal mass:

$$\rho_w = 2710 \frac{kg}{m^3} \quad c_w = .896(10^3)\frac{J}{kg\ K} \quad t_w = 28.7(10^{-6})\ m$$

$$2a = 3.18\ (10^{-3})m \quad \rho = 1.18 \frac{kg}{m^3} \quad \kappa = .222\ (10^{-4})\ m^2/s$$

$$c_p = 1.01\ (10^3)\ \frac{J}{kg\ K} \quad \bar{u} = 2.00\ m/s \quad \frac{\ell}{a} = 240$$

$$\alpha = 286 \text{ and if } f = .28 \text{ Hz then } \beta = .20$$

Then Re (Λ) = 6.59. Thus Re (X) = .0039 or about .39% reduction in amplitude.